P-T conditions and chemical changes of a vein and associated alteration in Monviso eclogites

Tyler Hicks

November 21, 2018

Advisors: Dr. Sarah Penniston-Dorland and William Hoover

GEOL394

Table of Contents

ABSTRACT

Fluids play an important role in processes that occur in subduction zones such as seismic events, creation of arc magma, and element cycling. The effects of fluids on rocks that form in subduction zones are studied by examining those that have been exhumed. In this study, an eclogite sample from the Monviso ophiolite in Italy is analyzed to understand processes and conditions of chemical transport by fluids in a subduction zone. Eclogites are high-pressure, low-temperature rocks dominated by garnet and omphacite and form in subduction zone environments. The eclogite sample that is analyzed consists mostly of omphacite and garnet. There is a vein that cuts through the rock, which is dominated by phengite, omphacite, and epidote, and is surrounded by an alteration selvage. Geothermobarometric results estimate the mineral rims in the host region crystallized from 451-587ºC at 2.4-2.9Gpa, while the mineral rims in the alteration selvage crystallized from 380-547ºC at 2-2.9Gpa which suggests that on average the alteration selvage must have crystallized at peak eclogite-facies conditions or just below peak conditions in the subduction zone. A bulk rock analysis of several cut slabs representing each of the main zones of the rock was performed to determine whether the alteration involved a change in chemical composition from fluid-rock interaction. A traverse from the host region to the vein as well as subsequent concentration ratio plots suggest that there is an enrichment in K, Rb, Cr, and Ni. These indicators suggest that components of the fluid were derived from a mix of both serpentinite and sedimentary lithologies, and the mixed fluid would have been present along the slab interface at the P-T conditions of the alteration.

I. INTRODUCTION

Subduction zones are locations where a number of societally important events take place, such as seismic activity and creation of arc volcanoes. Each of these events involves the presence of fluids. The release of dehydration fluids by high pore fluid pressure results in brittle behavior leading to seismicity (Audet, 2009; Hacker et al., 2003). They also cause melting of the overlying rock, creating arc magma that will rise and be expelled at the surface (Schmidt and Poli, 1998). Metamorphic rocks from subduction zones provide geoscientists with valuable information about the effect of fluids and chemical cycling. Exposed rocks provide information about where and when fluid-rock interaction is occurring and even the origin of the fluid(s). Additionally, the cycling of elements is better understood by studying rocks that interacted with fluids produced by devolatilization of the downgoing slab. It has been theorized that these fluids are mainly responsible for the transfer of elements into the overriding mantle and thus into arc magma that is brought to the surface (Spandler and Pirard, 2013). The reasons described above are several examples of why it is important to study fluids in subduction zones.

Metamorphic rocks, such as blueschist and eclogite, are high pressure, low temperature rocks that record relatively cool conditions in subduction zones due to the hydrated and subducted oceanic plate. These rocks have been exhumed from the subduction interface and throughout the subducting slab and sometimes show evidence for fluid interaction. Analyzing rocks that have been metasomatized or have veins provide information regarding the metamorphic conditions at which fluids interacted with the rock and the composition of the fluid itself. Metasomatism is defined as chemical changes within rocks induced by the interaction of hydrothermal fluids or an adjacent melt that leads to the crystallization of hydrous phases in the rock (Angiboust et al., 2014). The devolatilization occurring at elevated temperatures and pressures will release fluids which have the ability to organize into vein networks for fluid travel (Plümper et al., 2016). As hydrous phases break down, these fluids locally migrate through their source material (e.g. eclogite), until the additional breakdown of hydrous phases and formation of new phases such as garnet decrease the porosity of the rock leading to larger vein networks. When the fluids are released, they migrate between the downgoing slab and mantle wedge where they play an important role in element cycling. The migration of fluids carry elements that serve as indicators of a specific source such as oceanic sediments and serpentinites (van der Straaten et al., 2008; Spandler et al., 2011; Angiboust et al., 2014)

The Western Alps formed as a result of oceanic-continental plate subduction and subsequent collision. Near Monviso, located along the French-Italian border, there is an exposed piece of oceanic crust where many studies have been conducted investigating the effects of metasomatism and the associated metamorphic conditions (Groppo and Castelli, 2010; Spandler et al., 2011; Angiboust et al.,2012, 2014; Locatelli et al., 2018). These conditions have been estimated, however, the P-T conditions of veins and associated host rock have not been compared. This raises the question: At what conditions do fluids in the subduction zone interact with the rocks? Additionally what chemical changes are associated with the fluid that interacted with the rock, and what information can this provide regarding its origin.

The goal of this study is to estimate temperatures and pressures experienced by an eclogite sample that contains a vein and an alteration zone surrounding the vein from Monviso and put them in the context of previous P-T-time estimates for the region. Along with P-T estimates, chemical changes between the fluid and host rock is of interest to determine the source of the fluid that passed through. To address these goals, two hypotheses are generated: (1) the vein and alteration zone recrystallized at a lower pressure and temperature than the host rock; and, (2) the alteration zone adjacent to the vein is chemically different than the host rock due to the addition and/or loss of mobile elements from the interacting fluid.

II. GEOLOGIC BACKGROUND

The rock sample used in this study was collected from Monviso, Italy in the Western Alps (Fig. 1a). Located along the French-Italian border, the Monviso ophiolite is an intact section of eclogite-facies oceanic crust where geoscientists study fluid-induced metamorphism in subduction zones (Angiboust et al., 2012, 2014). Metamorphism of the rocks at Monviso occurred at roughly 50-40 Ma, before the European plate and part of the Tethyan oceanic crust subducted under the Apulian plate (Beltrando et al., 2010). A major unit of Monviso, the Lago Superiore Unit (LSU), is defined by a layer of serpentinites overlain by metagabbro and metabasalt and cut by eclogite-facies shear zones (Fig. 1b; Angiboust et al., 2014). The sample for this study was collected from the Lower Shear Zone (LSZ, Fig. 1b) which is characterized by eclogitic blocks in a serpentinite matrix. Two past studies of eclogites from the LSZ provide estimates of peak conditions from 550 ˚C at 2.7 GPa and 560-580 ˚C at 2.4-2.7 GPa (Angiboust et al., 2012; Locatelli et al., 2018). Additionally, there have been studies that have looked at the interaction of fluids with metasomatic rocks from this area that experience enrichment or depletion in certain elements based on the fluid composition. It has been found that some LSZ eclogites with enrichment in Cr and Ni as well as large ion lithophile elements (Cs, Rb, Ba, K) show implications for having interacted with fluids derived from a mixed serpentinite and a sediment-derived fluid (Angiboust et al., 2014).

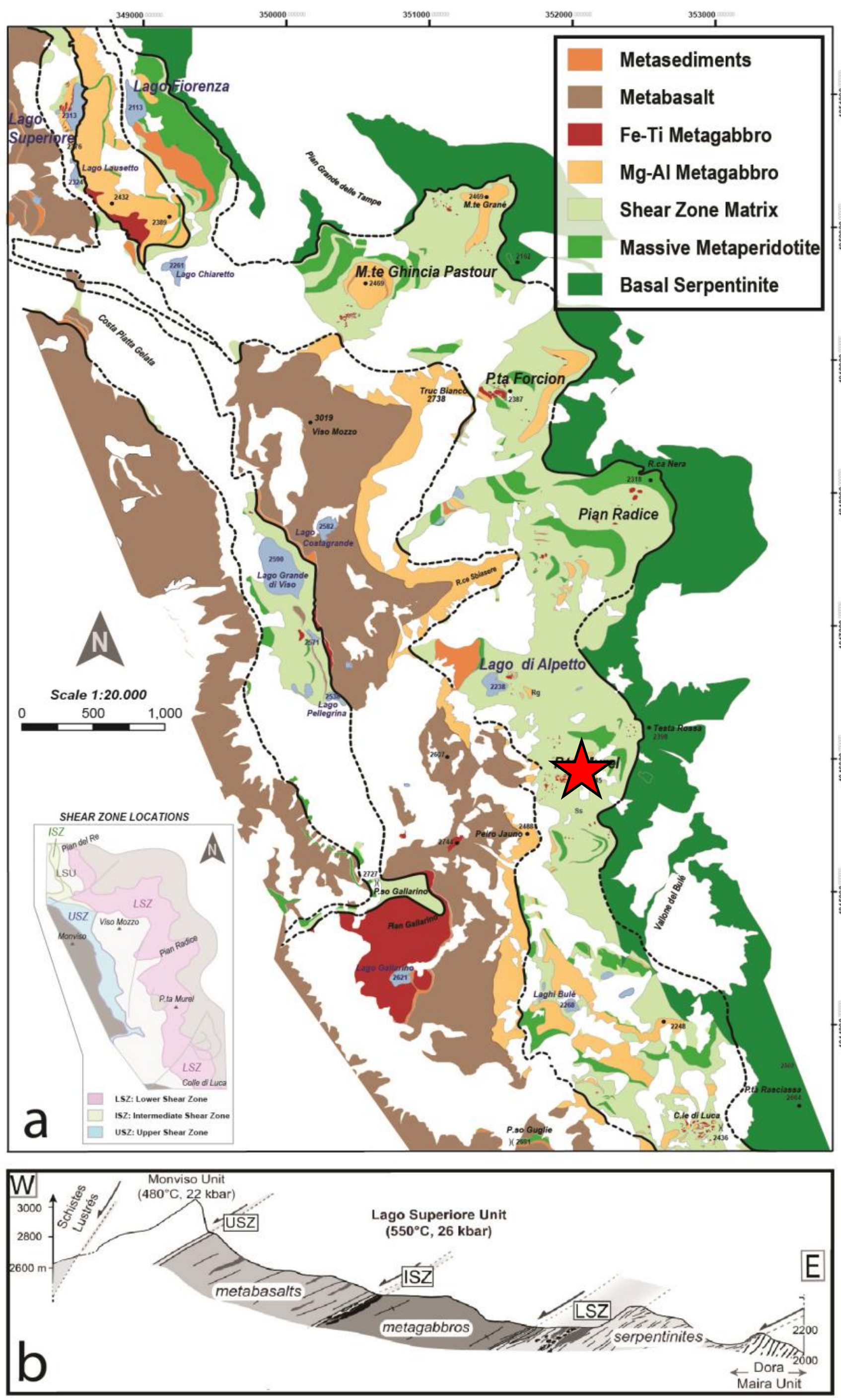

***Fig. 1**: (a) Geologic map of the Monviso ophiolite, Western Alps modified from Locatelli et al. (2018). Sampling site is indicated by the star. (b) Cross section across Monviso showing the LSU and LSZ above the zone of basal serpentinites and eclogitic blocks modified from Angiboust et al. (2012).*

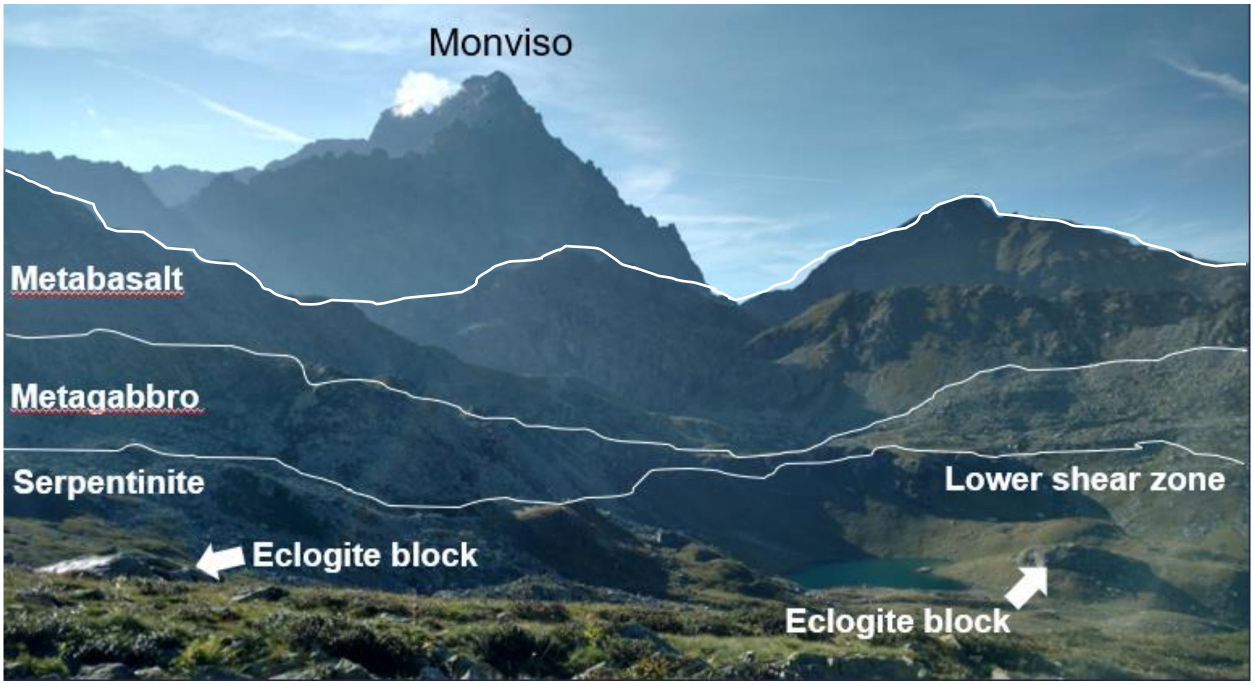

Fig. 2*: Field area of Monviso where the eclogite sample was collected from. The sample in this study was collected in the foreground of the photograph. Credit to Will Hoover.*

III. SAMPLE DESCRIPTION

The eclogite sample in this study is a piece of float that was collected near a large eclogitic block in the serpentinite matrix of the LSU, and can be divided into the host, alteration, and vein. Overall, host has the mineral assemblage of omphacite, garnet, phengite, and rutile. Omphacite is the main constituent of the matrix and cannot individually be seen without a microscope. In the host, there are many groups of small atoll garnets (garnets with inclusion rich cores). The alteration selvage has omphacite, garnet, glaucophane, and phengite, however the garnet here occurs as subhedral porphyroblasts that are few in number. The host rock is cut by a vein that shows a branching morphology, and is composed of phengite, omphacite, epidote, and apatite.

IV. METHODS

Provided below is a summary of the methods and techniques that are used in this study. Additional data tables are included in the appendix.

MINERAL ANALYSIS

Petrography

A total of five thin sections (Fig. 3) are used in this study, and together cover the major zones of the rock and their contacts. A Nikon Eclipse LV100 Polarizing microscope equipped with a QImaging Micropublisher 5.0 RTV camera provides insight into the major phases of the rock as well as mineral textures. Several photomicrographs were taken using plane-polarized light (PPL) and cross-polarized light (XPL; Fig. 5a-f) to document mineral assemblages of major phases in each major zone of the rock.

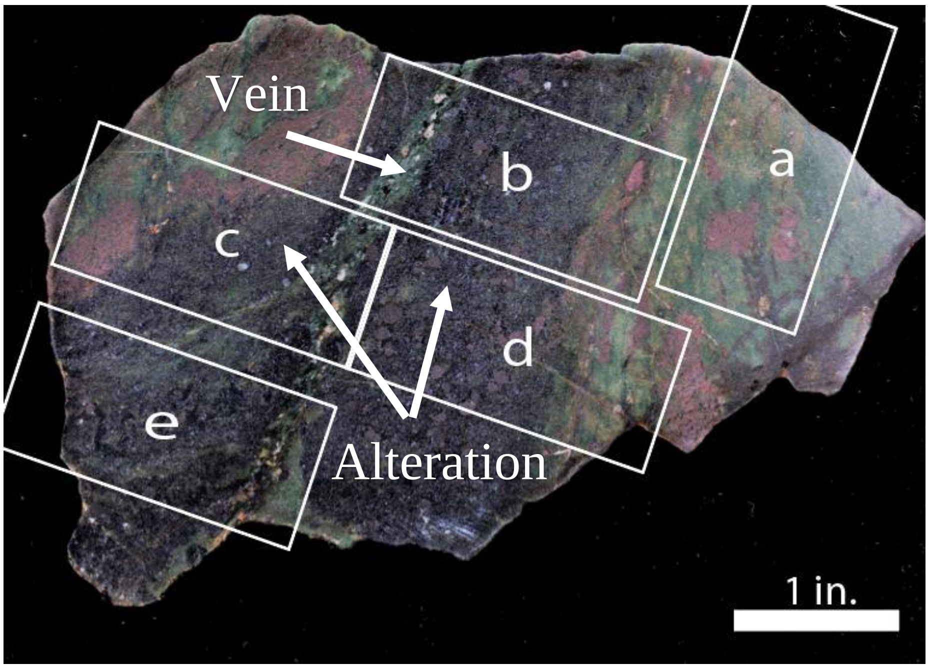

***Fig. 3**: Cut slab of sample showing the location of thin sections (a-e) in this study.*

MINERAL COMPOSITION

In this study, University of Maryland's JXA-8900 SuperProbe Electron Probe Microanalyzer was used under supervision by Dr. Phil Piccoli to analyze major and minor phases (grt, omp, phg) within the host, alteration zone, and vein. Operating conditions are an accelerating voltage of 15 kV, 10 nA cup current, 10μm beam diameter. For the analysis, multiple standards were used and are listed in Appendix 7. The correction program used for raw x-ray counts is Phi Rho Z. Elemental oxide data was processed and cation values are calculated for by normalizing to 12O for garnet, 8O for omphacite, and 11O for phengite. The filter for each analysis was 1.5 wt%.

BULK ROCK ANALYSIS

Major elements

X-ray Fluorescence Spectrometry was performed at Franklin and Marshall College. A total of 10 samples from the rock were cut; 5 from the host, 4 from alteration, and 1 from the vein. The size of the slabs that were cut were determined by the volume of the largest garnet porphyroblast, making sure the slab volume would be at least 100x that of the porphyroblast (Fig. 4). The cut slabs were crushed with a mortar and pestle and powdered with a shatter box. Powdered samples (0.4000 +/- 0.0001 grams) were sent to be analyzed for major elements. Each rock powder sample was mixed with 3.6000 +/- 0.0002 grams of lithium tetraborate and heated until molten. Once quenched, the samples were analyzed for SiO_2, Al_2O_3, CaO, K_2O, P_2O_5, TiO_2, Fe_2O_3, MnO, Na_2O, and MgO with the use of the PANalytical 2404 X-ray fluorescence vacuum spectrometer. Geochemical standard BHVO-2 was analyzed by XRF for major and trace elements to assess accuracy and precision (<1%) (Franklin and Marshall College; Appendix 6).

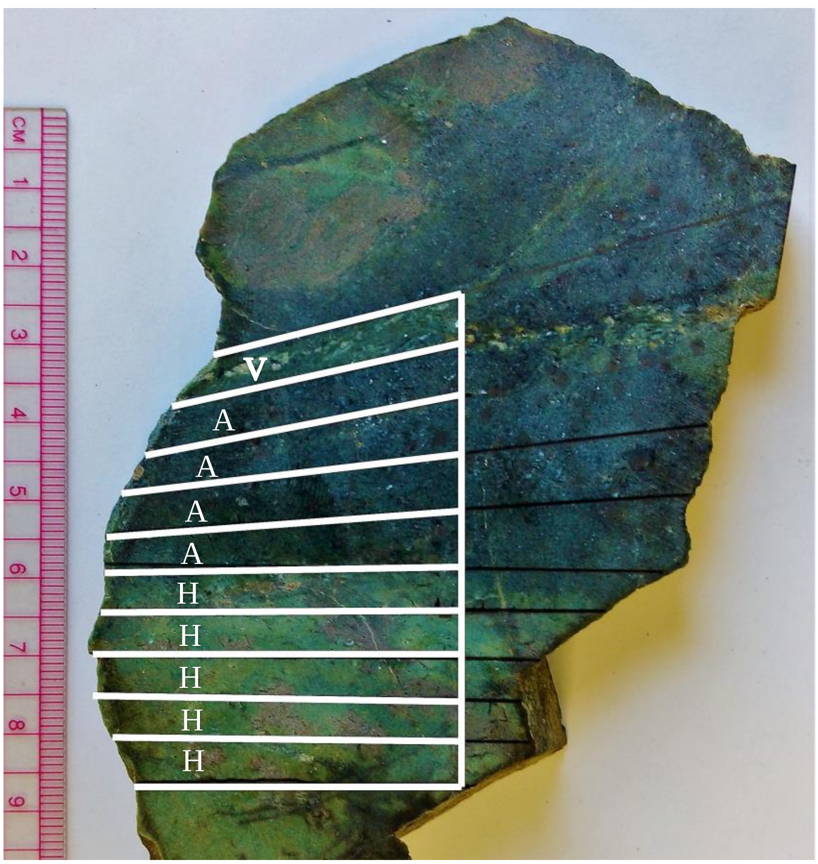

***Fig. 4**: Cut slab of sample showing the location of slices taken for bulk rock geochemical analysis, where V is vein, A is alteration, and H is host.*

Trace elements

Trace element analysis was performed at the University of Maryland, using the Element 2 Inductively Coupled Plasma Mass Spectrometer (ICP-MS) under the supervision of Dr. Richard Ash. About 20mg of rock powder from each of the ten cut slabs was weighed out (see Appendix 8). For methods and operating conditions see Filiberto et al. (2018). Rock powders were dissolved in screw-top Savillex beakers on a hot plate using step additions of concentrated HF, HNO3, and HCl acid with dry downs in between until solutions were clear. Solutions were doped with Indium and then diluted in 0.8M HNO3; the total dilution of the rock powder to what was measured was a 15150 dilution. The geochemical standard BHVO-2 was used alongside the ten samples being analyzed.

ANALYSIS OF UNCERTAINTY

Electron Probe

Uncertainty from counting statistics was determined for garnet, omphacite, and phengite in which $1\sigma=\sqrt{N}/N*100$, where N= # of counts (see Appendix 1d-1f). The error is given in percent of the calculated weight percent (wt%).

Major and Trace Elements

Measurements of precision and accuracy were conducted by Franklin & Marshall College with the universal basalt standard BHVO-2 (See Appendix 6). Percent relative uncertainty for major elemental oxides is calculated at the 2σ level and can be seen in Table 1 below. Trace element uncertainty is calculated using the uncertainty of accepted values of GeoReM BHVO-2 samples from Jochum et al., (2007) which are located in Appendix 5.

Oxide	**SiO2**	**TiO2**	**Al2O3**	**Fe2O3T**	**MnO**	**MgO**	**CaO**	**Na2O**	**K2O**	**P2O5**
% Relative Uncertainty 2σ	0.18	0.00	0.30	0.15	0.84	0.19	0.13	0.47	0.66	1.27

Table 1: Percent relative uncertainty of major elemental oxides calculated using BHVO-2 test for accuracy and precision data found in the appendix.

V. RESULTS

PETROGRAPHIC ANALYSIS

Host Rock

The host rock is dominated by omphacite and garnet, with few phengite grains throughout. Garnet in this section appear small (0.1-0.15mm), euhedral, and with inclusion-rich cores. Omphacite present here dominates matrix and appear as grains <0.1mm. Phengite, which appears as elongate porphyroblasts (0.8mm) with smooth grain boundaries are few in number. Rutile occurs in the host as small blobs (<0.1mm) in the matrix and as inclusions within phengite and garnet.

Alteration Zone

The presence of glaucophane signifies the transition from host to alteration. Glaucophane appears mostly as euhedral grains (0.7-1.35mm) that are present all throughout the alteration. Omphacite continues to dominate the matrix, and phengite in similar abundance to the host as elongate porphyroblasts. Garnet in the alteration appears as porphyroblasts (1.5-2mm) with a poikilitic texture, and appear to be partially corroded around the outer rim. Rutile occurs similarly as it does in the host, as small (<0.1mm) blobs in the matrix and inclusions in garnet, phengite, and glaucophane.

Vein

Phengite is abundant in the vein, and appear as larger subhedral porphyroblasts up to 1mm in length. Omphacite, epidote, and apatite are also found throughout, but in smaller quantities. Garnet and glaucophane are absent in the vein. Rutile is rarer in the vein relative to the host and alteration.

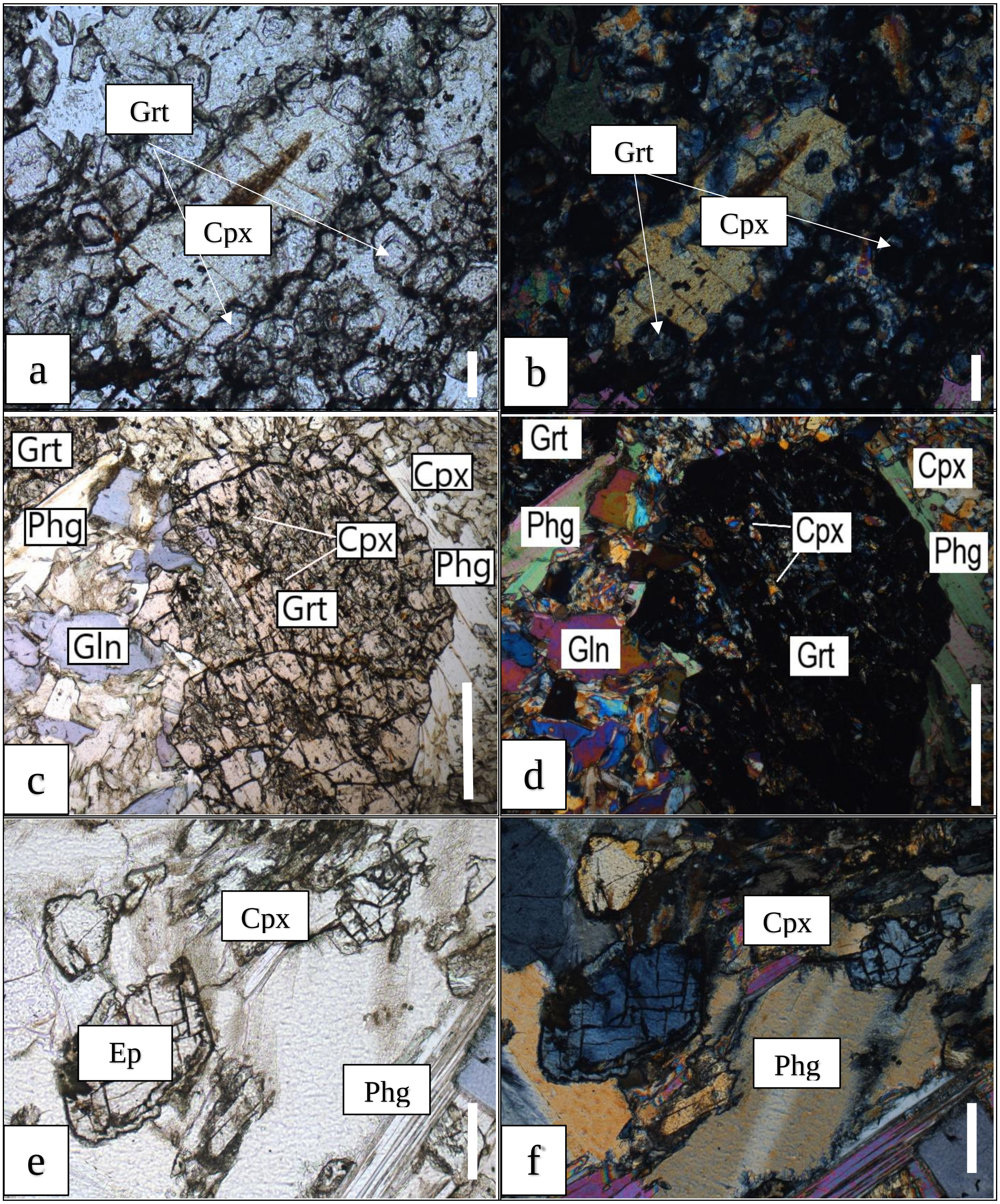

Fig. 5*: Photomicrographs of assemblages for petrography: (a) Host assemblage (PPL); (b) Host assemblage XPL; (c) Alteration assemblage (PPL); (d) Alteration assemblage (XPL); (e) Vein assemblage (PPL); (f) Vein assemblage (XPL). Scale bars are set to 0.1mm in a-b, 0.5mm in c-d. Phg: Phengite, Cpx: Clinopyroxene, Ep: Epidote, Grt: Garnet.*

MINERAL COMPOSITIONS

Garnet rims are Fe-rich and were averaged for P-T calculations. Garnet points in the alteration are similar in chemistry to those in the host, and the composition is relatively homogeneous (see Appendix 1a); the most variable cation is Ca and has wt% values that range from 2.57-4.33 wt%. Magnesium also varies a little, ranging from 4.84-6.39 wt%. Omphacite rims are Na-Al-rich and show variability in the host and alteration (see Fig. 7 and Appendix 1b); the most variable cation is Fe and has values that range from 5.55-10.60 wt%. The phengite grains analyzed are also variable throughout the sample (see Fig. 8 and Appendix 1c), with Al having the highest variability from values ranging from 18.7-26.41 wt%. Those that are from the alteration also have higher K to Si ratio also seen in Fig. 8.

.

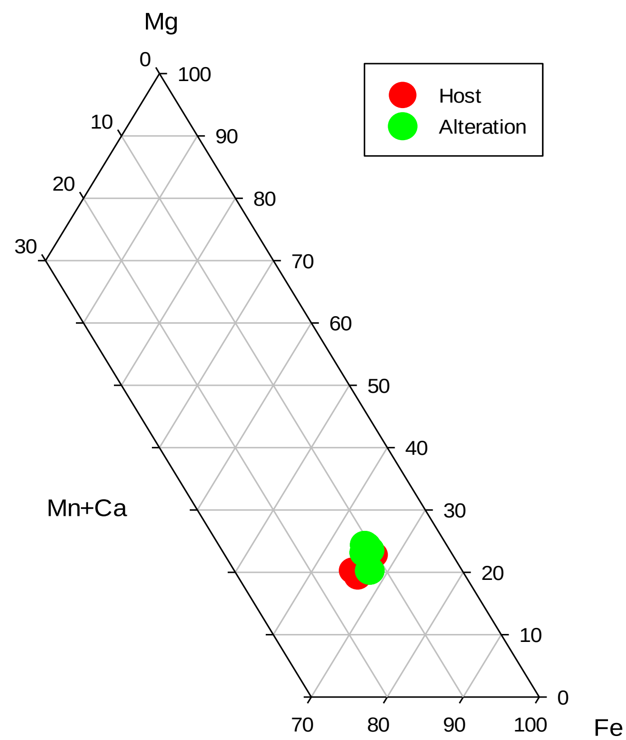

Fig. 6*: Ternary plot for garnet grains in the used for geothermobarometry estimates.*

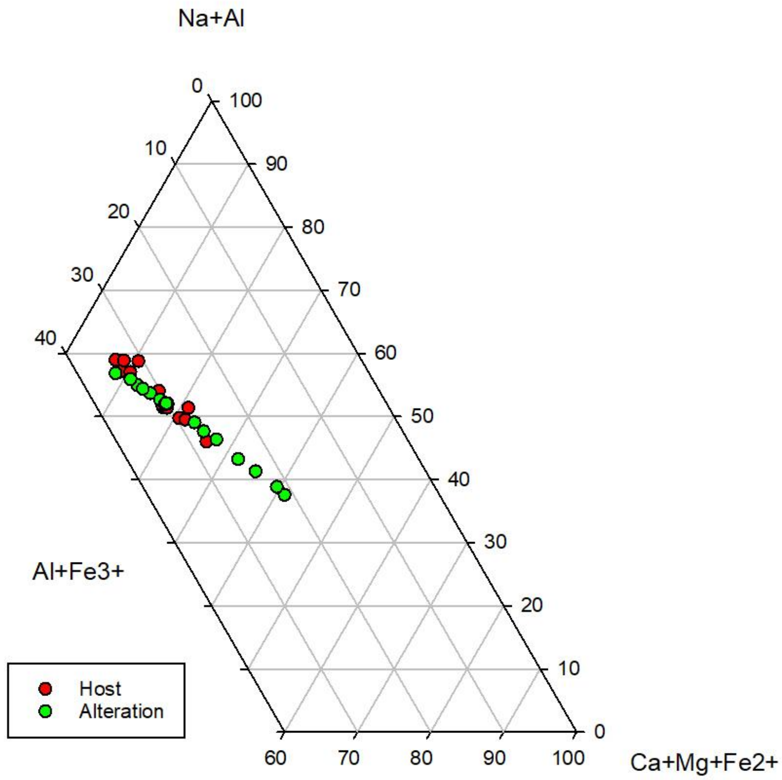

Fig. 7: Ternary plot of variable omphacite grains used in geothermobarometry estimates. Na+Al: Jd; Al+Fe3+: Aeg; Ca+Mg+Fe2+: En, Fs, Wo.

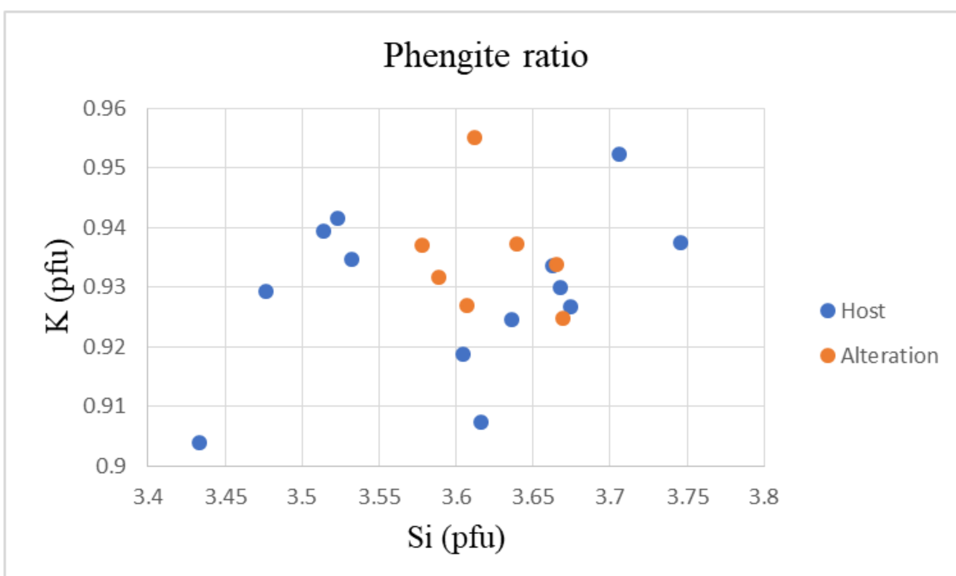

***Fig. 8**: Ratio of Si to K in per formula unit (pfu) of variable phengite grains used in geothermobarometry estimates.*

BULK ROCK ANALYSIS

Major and Trace Elements

Moving across the host to the vein, there is variability in most elements. However, the most systematic changes from host to alteration are an increase in Mg and K and decreases in Na, Mn, and P. The host also appears to be more Na-rich than the alteration. Compared to major elements, there is more variability in the trace elements present from the host rock to the vein. Figures 11-14 show concentration in ppm of trace elements analyzed with the Element 2. Most systematic changes from host to alteration are an increase in Ni, Cr, and Rb and decreases in REE, Zr, Pb, Nb, Th, and Ta. Elements with the lowest variation include U and W.

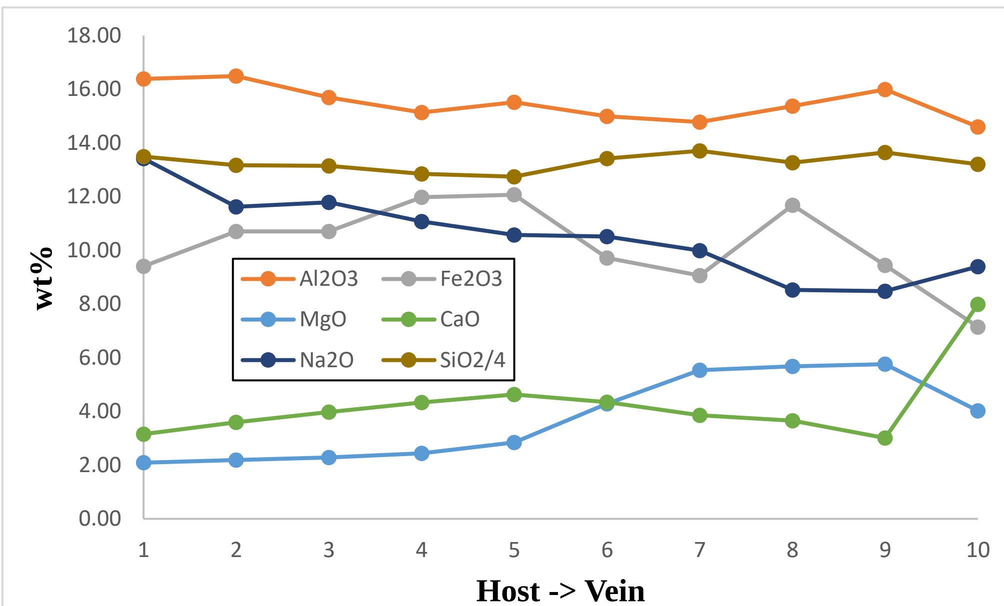

Fig. 9*: Plot of high concentration (wt%) major elements from host (1-5), alteration (6-9), and vein (10).*

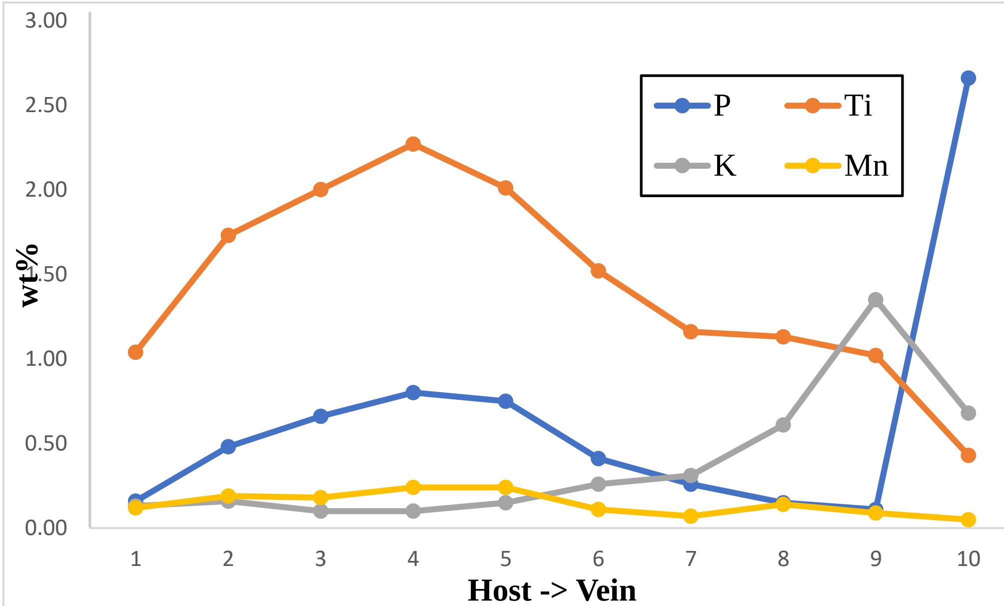

Fig. 10*: Plot of low concentration (wt%) major elements from host (1-5), alteration (6-9), and vein (10).*

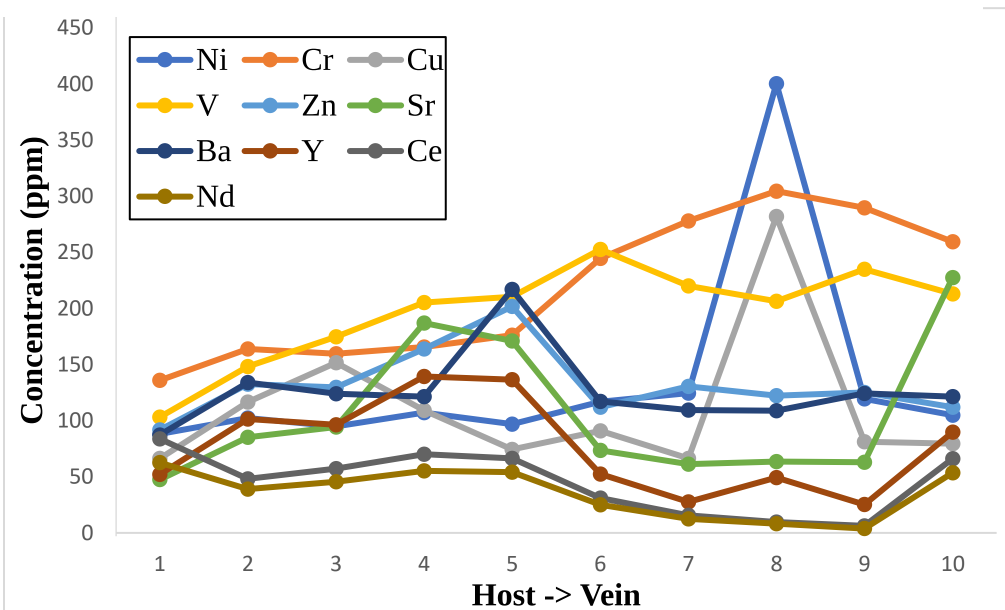

Fig. 11*: Traverse of varying trace element (Ni, Cr, Cu, V, Zn, Sr, Ba, Y, Ce, Nd) concentrations from host (1-5), alteration (6-9), and vein (10).*

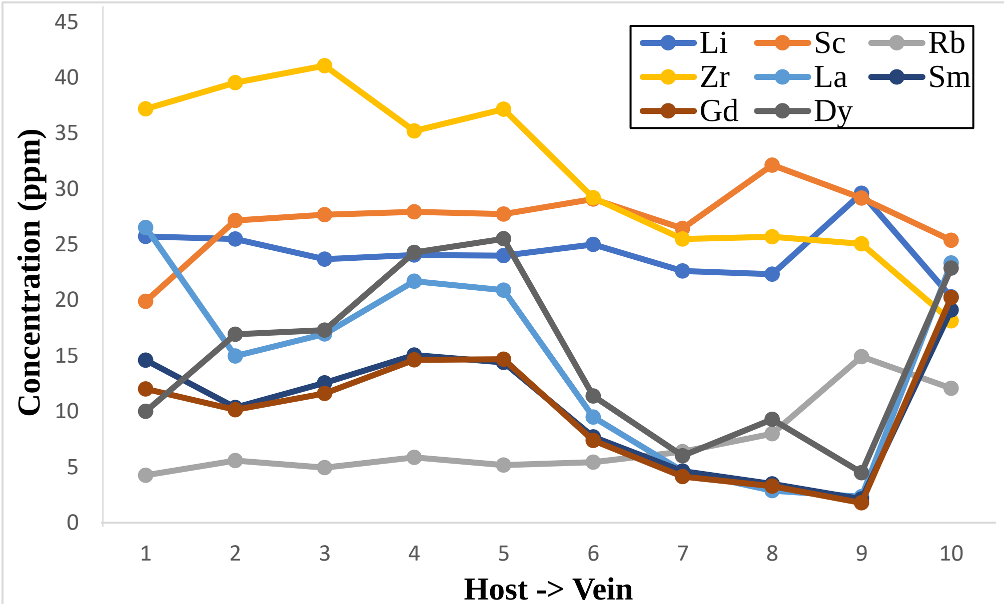

Fig. 12: *Traverse of varying trace element (Li, Zr, Gd, Sc, La, Dy, Rb, Sm) concentrations from host (1-5), alteration (6-9), and vein (10).*

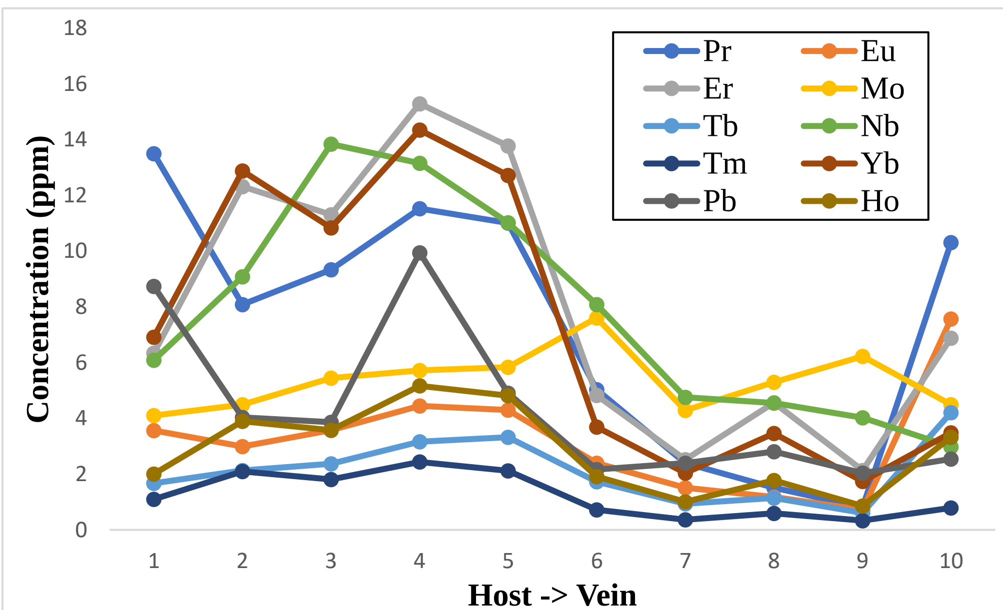

Fig. 13*: Traverse of varying trace element (Pr, Eu, Er, Mo, Tb, Nb, Tm, Yb) concentrations from host (1-5), alteration (6-9), and vein (10).*

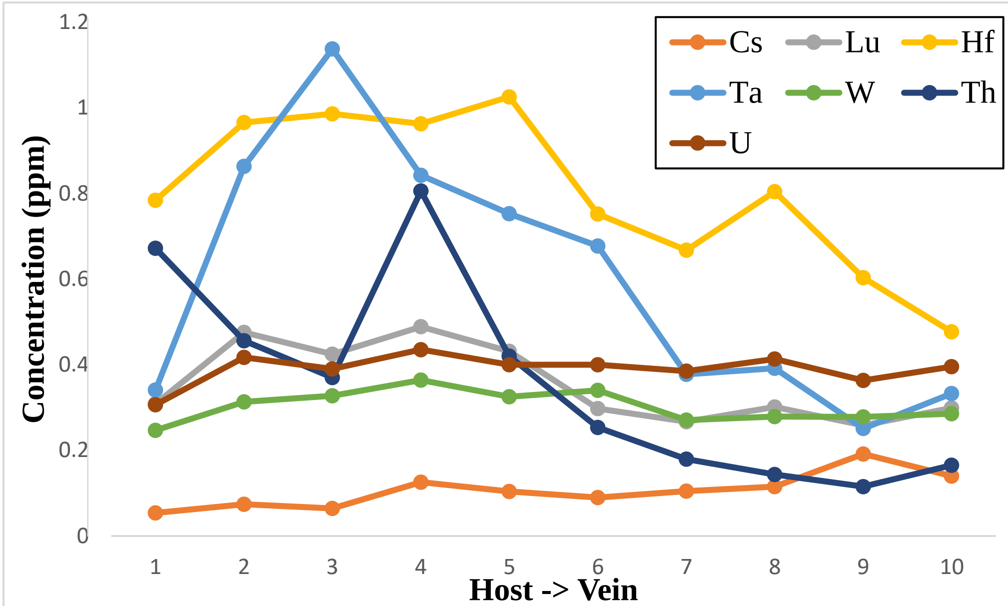

Fig. 14: *Traverse of varying trace element (Cs, Lu, Hf, Ta, W, Th, U) concentrations from host (1-5), alteration (6-9), and vein (10).*

VI. DISCUSSION

P-T CONDITIONS

Pressure-temperature calculations for the host and alteration utilize assemblages of garnet, omphacite, and phengite in equilibrium, and contact where possible (See Appendix 10). The garnet-clinopyroxene Fe^{2+}-Mg geothermometer (Ravna, 2000) expression below was used in this study to estimate temperature and pressure of the host and alteration zone. The thermometer uses garnet and clinopyroxene wt% compositions of Ca, Mg, and Fe (Ravna, 2000).

$$T(^{\circ}C) = [(1939.9 + 3270X_{Ca}^{Grt} - 1396(X_{Ca}^{Grt})^2 + 3319X_{Mn}^{Grt} - 3535(X_{Mn}^{Grt})^2 + 1105X_{Mg\#}^{Grt} - 3561(X_{Mg\#}^{Grt})^2 + 2324(X_{Mg\#}^{Grt})^3 + 169.4P(GPa))/(\ln K_D + 1.223)] - 273;$$

where X_b^a is the mole fraction of element b in mineral a; K_D is the distribution coefficient; and P is pressure in GPa. In this study, pressure is calculated using the Waters and Martin (1996) garnet-clinopyroxene-phengite geobarometer expression below:

$$P(kbar) = 28.05 + 0.02044T - 0.002995Tln(k);$$

where P is pressure in kbar, T is temperature in K (Kelvin), and k is an equilibrium constant following the calibration definitions of Waters and Martin (1996). The calibration is based on the dataset provided by Holland and Powell (1990) and assumes ideal mixing on site for phengite as well Mg-Ca mixing for garnet.

Uncertainty on the geothermometer is discussed in Ravna (2000), where 27 datasets with 311 data pairs are combined with 49 natural Mn-rich samples to calculate a range of temperature values (see Ravna, 2000). Using experimental values from these datasets, the geothermometric expression from Ravna (2000) produces temperatures within +/- 100˚C. There are a number of datapoints from the host and alteration that overlap, but the average host conditions are higher than the average alteration conditions. Additionally, these overlaps in the data are acceptable considering they are within uncertainty of the geothermometer. For barometry, the Waters and Martin (1996) geobarometer does not explicitly state the uncertainty of pressure estimates using the calibration offered. However, it has been found that typical uncertainties on geobarometers are $\pm$1kbar (Whitney, 2016).

For this analysis grt-omp-phg samples were used from the host and alteration. In the host, peak temperatures are calculated at 469-587ºC, while peak pressures are calculated at 2.4-2.9GPa. The alteration experienced temperatures at about 380-547ºC with pressures from 2-2.9Gpa (Tables 2-3, Fig. 15), which is slightly lower and more variable than the host rock estimates. Overall, there were 8 P-T estimates for the host and 17 for the alteration (Tables 2-3). A complete table of all P-T calculations considered in this study can be found in Appendix 4. Some estimates resulted in calculated temperatures and pressures that are geologically unreasonable (e.g. 760-798ºC and 3.6-4.3GPa) because they are outside the stability fields of the existing mineral assemblage and in some cases above the melting temperatures of these rocks.

Sample	T(ºC) +/-100ºC	P(Gpa) +/-0.1GPa
Host 1	539, 539, 539	2.8, 2.8, 2.9
Host 2	584, 587, 574	2.6, 2.6, 2.4
Host 3	469	2.4

***Table 2**: Pressure-temperature estimates for Host 1-3.*

Sample	T(ºC) +/-100ºC	P(Gpa) +/-0.1GPa
Alteration 1	437, 436, 441, 439, 426, 425	2.1, 2.1, 2.1, 2.1, 2.1, 2
Alteration 2	522	2.9
Alteration 3	441, 438, 547, 544	2.1, 2.1, 2.8, 2.7
Alteration 4	467, 474, 380, 385, 487, 494	2.2, 2.4, 2, 2.2, 2.4, 2.6

***Table 3:** Pressure-temperature estimates for Alteration 1-4.*

The peak P-T conditions for the alteration zone overlap with those of the host rock but are on average lower than the host. This suggests that the vein and its associated alteration zone formed at or near the peak metamorphism of the host rock. However, the hottest host estimate and coldest alteration estimate do not overlap in uncertainty, and therefore for only this set of data can it be suggested that there is a significant difference in host and alteration conditions.

Estimated temperatures and pressures for the host rock are similar to the unaltered eclogites in this region from other studies (see Fig. 15 using estimates from Groppo and Castelli, (2010); Angiboust et al., (2012), Locatelli et al., (2018)). Temperatures estimated by Groppo and Castelli (2010) using metagabbros from the LSU range from 420ºC, 16 kbar (1.6GPa) to peak conditions of 550ºC, 25-26 kbar (2.5-2.6GPa) and show a prograde path of conditions experienced by the rocks. An additional P-T estimate for metagabbros from the LSU was estimated at 550ºC, 26–27 kbar (2.6-2.7GPa) by Angiboust et al., (2012). Just recently, there was a study that looked at three different sections of an eclogite breccia, one being a zone of omphacite and garnet, similar to the unaltered zone of the eclogite being considered here. Estimates of this similar zone are 560 °C, 2.4GPa (Locatelli et al., 2018).

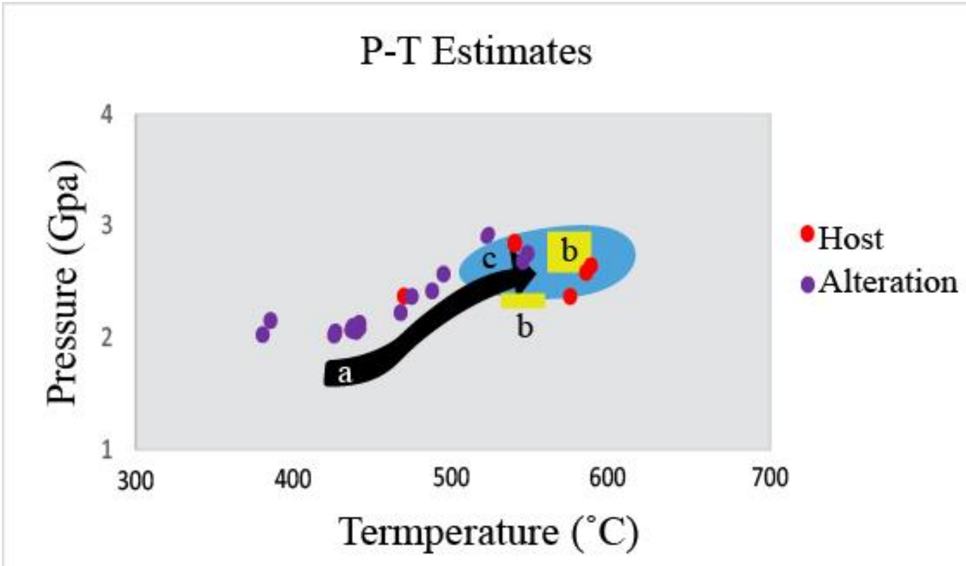

***Fig. 15**: Pressure-Temperature plot with host and alteration (red and purple respectively) compared against (a) Groppo and Castelli (2010), (b) Locatelli et al. (2018), and (c) Angiboust et al. (2012, 2014).*

BULK ROCK ANALYSIS

Mass balance

Mass change is quantified under the assumption that there is no volume change across the host and alteration since there is no evidence in mineral textures for a volume change and no consistent changes in concentration of relatively immobile elements such as Zr, Ti and REE (see Penniston-Dorland and Ferry, 2008) in the alteration zone compared to the host rock that would be suggestive of volume change. Figure 16 shows ratios of the concentrations of major elements in the host rock to the host rock average concentration. The graph illustrates the variation for each major element in the host rock. This variation is due to the natural rock heterogeneity and provides a framework to evaluate variations in the alteration zone. The bars plotted on this diagram show upper and lower bounds that are taken as the uncertainty due to natural rock heterogeneity and are included on a similar concentration ratio graph for major elements in the alteration zone. Ratios that fall outside these bounds suggest either addition of an element during alteration (above the range) or depletion of an element during alteration (below the range).

Mass balance figures 16-21 show that the alteration is enriched in K, Mg, Ni, Cr, and Rb and depleted in REE, Pb, Th, Y, and Mn relative to the average host rock. The addition of Mg, Ni and Cr are indicative of a serpentinite fluid source and the addition of K and Rb are indicative of a sedimentary fluid source (Angiboust et al., 2014). Since the alteration exhibits the addition of these elements, this tells us that the fluid is likely a mixture derived from both of these rock types. Given the results for mass balance, it’s suggested that during the exhumation of the large piece of oceanic crust, a mix of serpentinite and sedimentary derived fluids were present along the slab interface at the P-T conditions of the alteration (380-547ºC, 2-2.9Gpa).

Many studies have looked at compositional changes due to fluid-rock interaction which are recorded by metamorphic rocks from subduction zones (Angiboust et al., 2014; Beinlich et al., 2009; Groppo and Castelli, 2010; Li et al., 2017; Van der stratten, 2008). Eclogites with metasomatic rinds from the LSZ of the LSU were found to have been enriched in Mg, Cr, Ni, and large ion lithophile elements (LILE; Angiboust et al., 2014), which is similar to the compositional enrichments in the alteration zone of the rock used in this study that also show enrichments in Mg, Cr , Ni, and LILE (Pb, Rb). However, in the same study most of the LSZ samples exhibited a depletion in V which contrasts with the very slight enrichment of V in the alteration zone. The Mn enrichment can be explained by its transport from the breaking down of garnet and omphacite into other crystal lattices (Angiboust et al., 2014). A study conducted by Beinlich et al. (2009) on blueschists with eclogite selvage in the Tianshan mountains of western China also similarly found enrichment in LILE within a blueschist host, explained by the breakdown of phengite as eclogite facies conditions are reached. This gives a new perspective on the LILE enrichment that we see in the alteration zone in the rock for this study; it is possible that the LILE enrichment is due to the breakdown of phengite, indicating that during exhumation the rock may have experienced elevated metamorphic conditions after vein formation. An additional study of fluid-rock interaction and mass transfer in the Tianshan Mountains was conducted by Li et al. (2017) and looked at a blueschist sample with a glaucophane-phengite vein cutting through it. Mass balance results yielded additions of LILE (Rb, K, Pb) and a loss in Mn, Y, and REE which is consistent with results from the Monvoso eclogites. However, the loss of Mn, Y, and REE is said to be attributed to the dissolution of garnet in the blueschist host due to fluid-rock interaction. This would explain the similar loss of these elements in the alteration zone of the eclogite rock from Monviso.

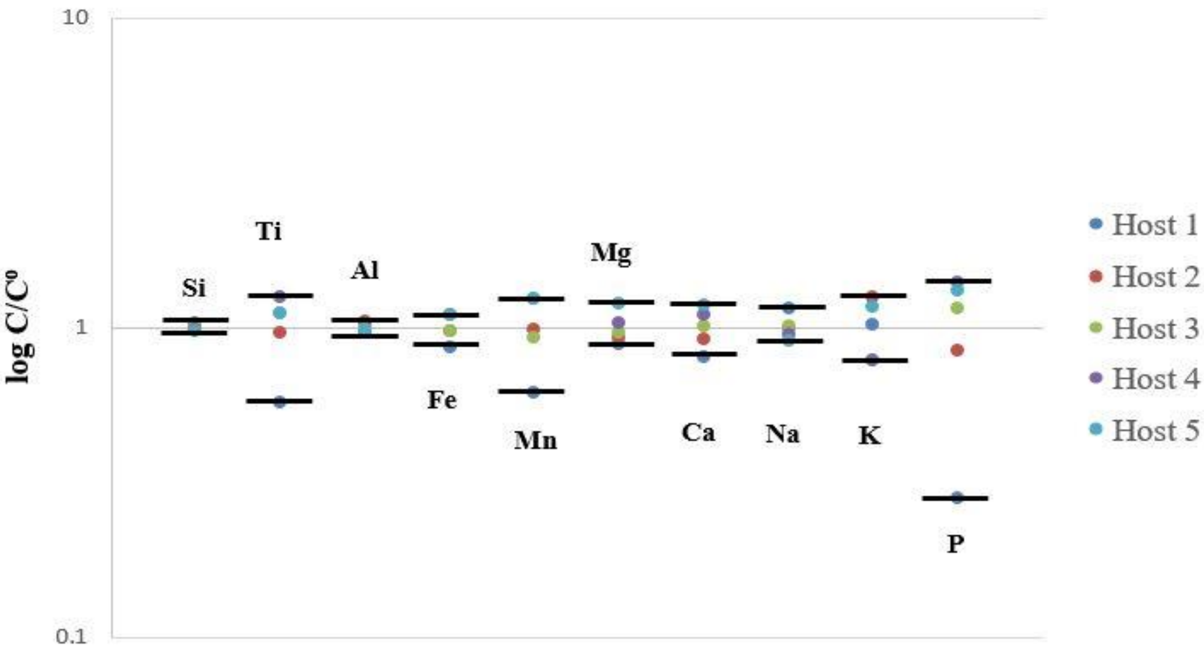

Fig. 16*: Concentration ratios (log scale) of major elements in the host. The horizontal line at 1 represents no mass change.*

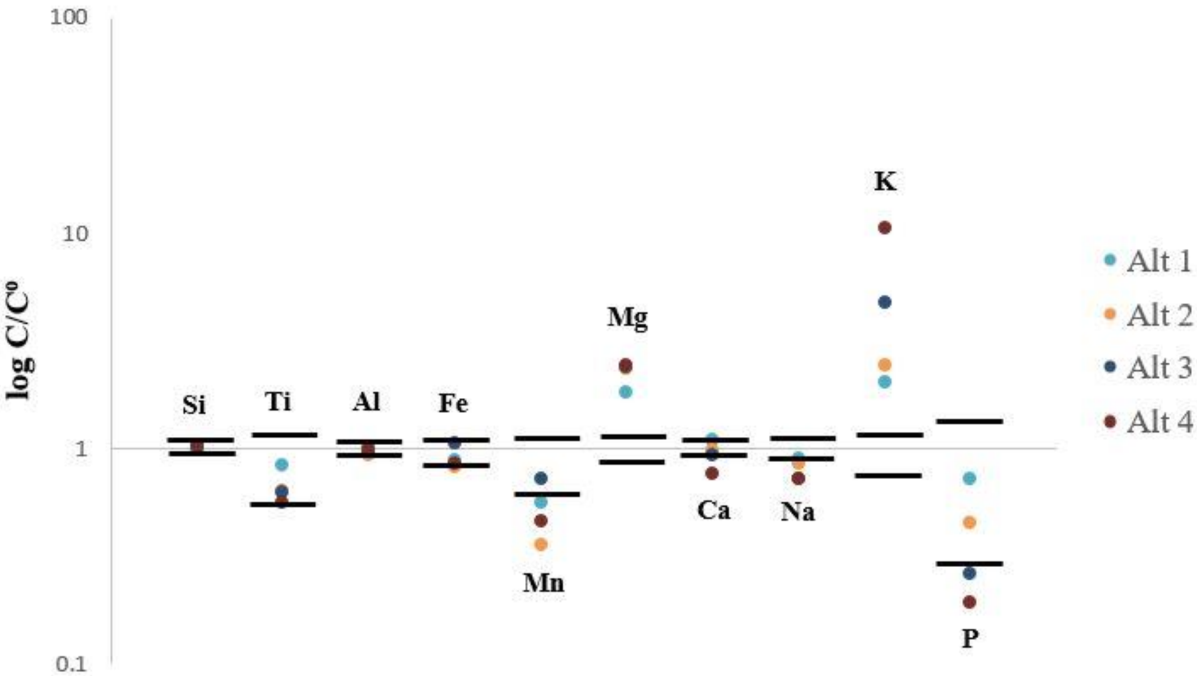

Fig. 17*: Concentration ratios (log scale) of major elements in the alteration. The horizontal line at 1 represents no mass change.*

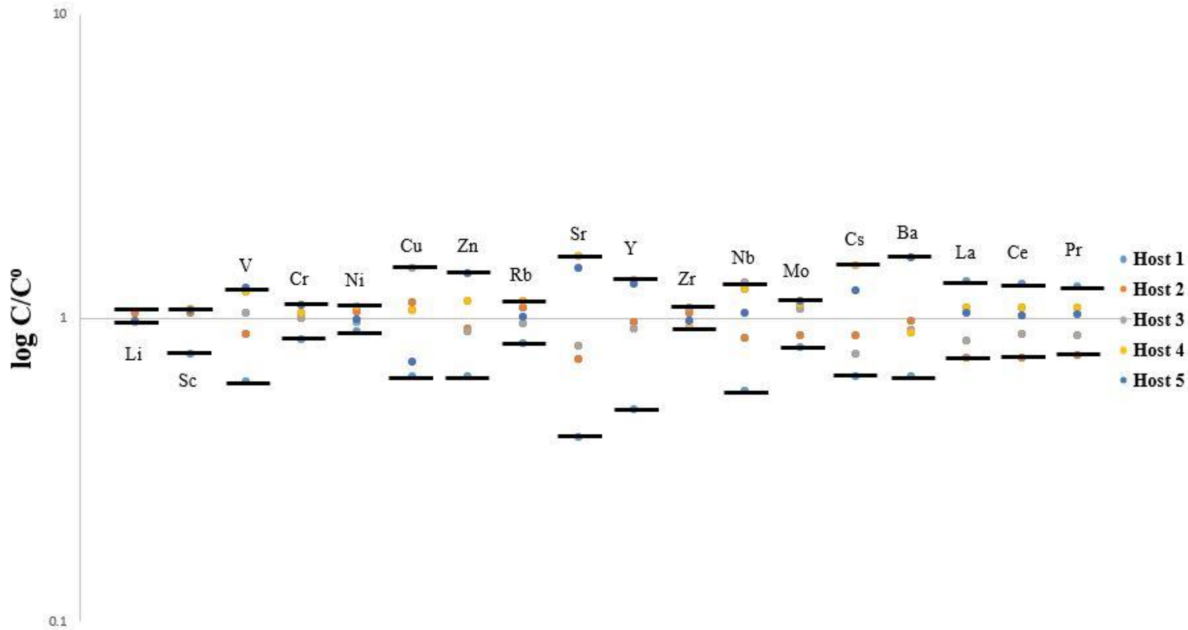

Fig. 18*: Concentration ratios (log scale) of the first 18 trace elements in the host. The horizontal line at 1 represents no mass change.*

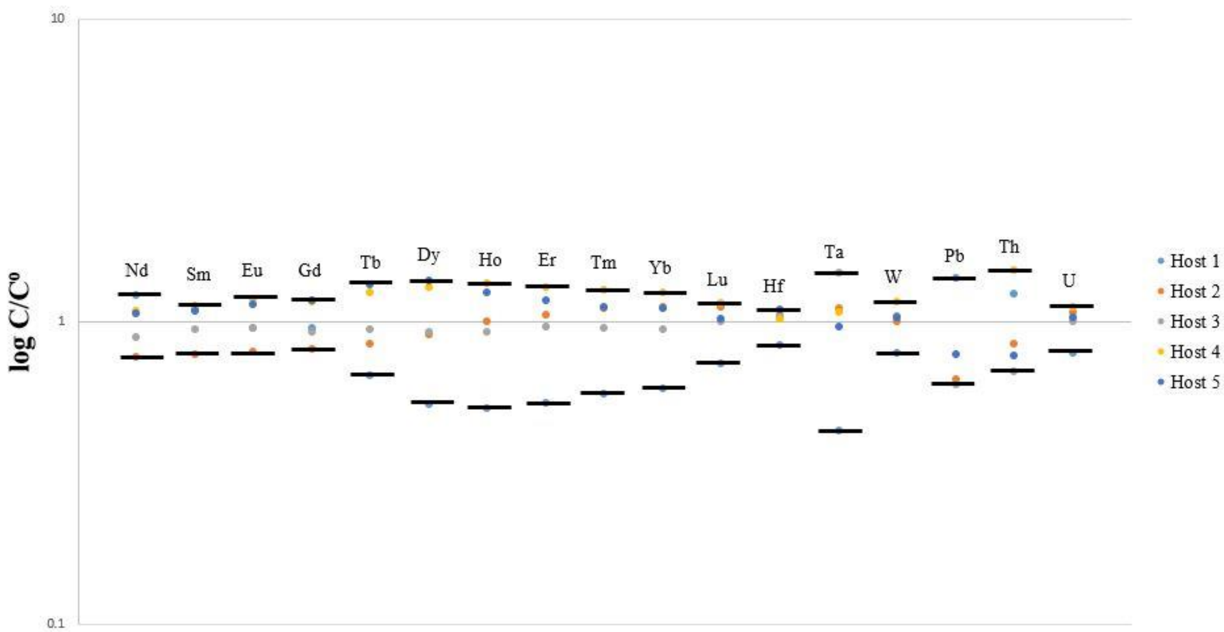

Fig. 19*: Concentration ratios (log scale) of the next 17 trace elements in the host. The horizontal line at 1 represents no mass change.*

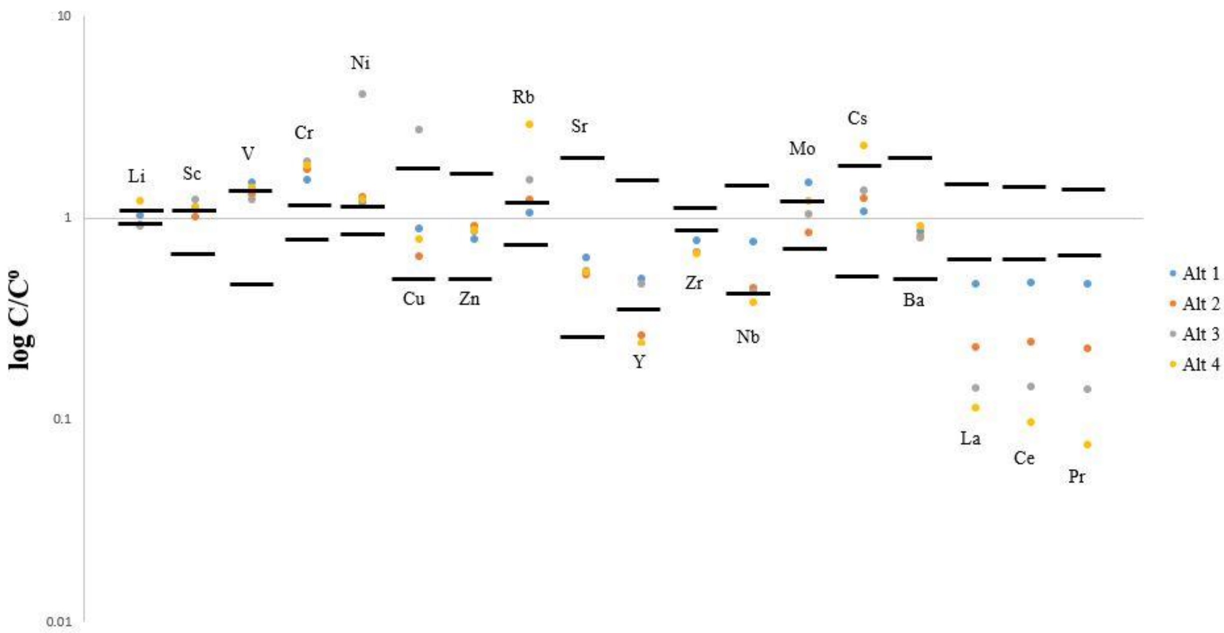

Fig. 20: *Concentration ratios (log scale) of the first 18 trace elements in the alteration. The horizontal line at 1 represents no mass change.*

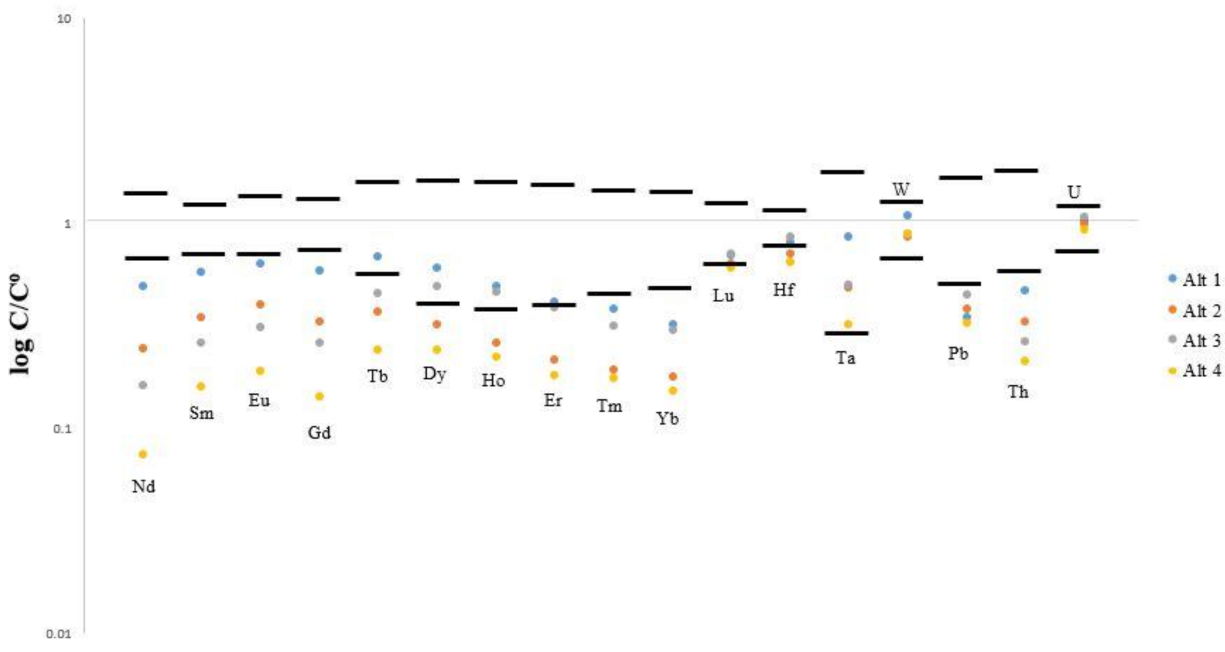

Fig. 21*: Concentration ratios (log scale) of the next 17 trace elements in the alteration. The horizontal line at 1 represents no mass change.*

VII. CONCLUSIONS

An eclogite from the Monviso ophiolite was collected from the field and analyzed for pressure-temperature conditions and chemical composition. The vein and alteration selvage present in the rock are mineralogically different than the host, and yield varying P-T conditions. Assemblages of garnet, omphacite, and phengite were used to estimate temperatures and pressures of the host and alteration zone. The Grt-cpx-phg Geobarometer (Waters and Martin, 1996) yields temperatures for the host from 451-587ºC and the alteration from 380-547ºC, while the Grt-cpx Geothermometer (Ravna, 2000) yields pressures at 2-2.9Gpa for the host and 2.4-2.9Gpa for the alteration. Bulk rock analysis suggests interaction with a fluid of mixed lithology by changes in composition from host to vein. The alteration selvage is enriched in K, Mg, Ni, Cr, and Rb and depleted in REE, Pb, Th, Y, and Mn. The enrichment of K and Rb suggest a sedimentary derived fluid while Ni, Cr, and Rb suggest a serpentinite derived fluid.

VIII. ACKNOWLEDGEMENTS

This paper has benefitted from the unwavering support of Sarah Penniston-Dorland and William Hoover over the course of the past year. Their advices for my research proved to be a landmark effort towards the success of my project. Philip Piccoli is acknowledged for providing guidance through the senior thesis process and support with the use of the Electron Probe Microanalyzer. Richard Ash is thanked for the use of the Element 2 Inductively Coupled Plasma-Mass Spectrometer and guidance for trace element analysis. Stanley Mertzman of Franklin & Marshall College is acknowledged for the preparation of the rock powdered samples and collection of bulk major element analysis data. Family and friends are also acknowledged for their motivation and continuous support of my efforts.

IX. BIBLIOGRAPHY

1. Angiboust, S.; Langdon, R.; Agard, P.; Waters, D.; and Chopin, C. (2012). Eclogitization of the Monviso ophiolite (W. Alps) and implications on subduction dynamics. Journal of Metamorphic Geology 30, 37-61.
2. Angiboust, S.; Pettke, T.; De Hoog, J.; Caron, B.; and Oncken, O. (2014). Channelized Fluid Flow and Eclogite-facies Metasomatism along the Subduction Shear Zone. Journal of Petrology 55, 883-916.
3. Audet, P.; Bostock, M.G.; Christensen, N.I.; and Peacock, S.M. (2009). Seismic evidence for overpressured subducted oceanic crust and megathrust fault sealing. Nature 457, 7225, 76-78.
4. Beltrando, M.; Compagnoni, R.; and Lombardo, B. (2010). (Ultra-) High-pressure metamorphism and orogenesis: An Alpine perspective. Gondwana Research 18, 147-166.
5. Beinlich, A.; Klemd, R.; John, T.; Gao, J. 2010. Trace-element mobilization during Ca-metasomatism along a major fluid conduit: Eclogitization of blueschist as a consequence of fluid–rock interaction. Geochimica et Cosmochimica Acta 74, 6, 1892-1922.
6. Filiberto, J; Gross, J.; Udry, A.; Trela, J.; Wittmann, A.; Cannon, K. M.; Penniston-Dorland, S.; Ash, R.; Hamilton, V. E.; Meado, A. L., Carpenter, P; Jolliff, B.; and Ferré, E. C. (2018). Shergottite Northwest Africa 6963: A Pyroxene-Cumulate Martian Gabbro. Journal of Geophysical Research: Planets 123, 1823–1841.
7. Hacker, B.R.; Peacock, S.M.; Abers, G.A.; Holloway, S.D. (2003). Subduction factory - 2. Are intermediate-depth earthquakes in subducting slabs linked to metamorphic dehydration reactions? Journal of Geophysical Research-Solid Earth 108, B1, 2030.
8. Holland, T.J. and Powell, R. (1990). An enlarged and updated internally consistent thermodynamic dataset with uncertainties and correlations: the system K_2O-Na_2O-CaO-MgO-MnO-FeO-Fe_2O_3-Al_2O_3-TiO_2-SiO_2-C-H_2-O_2. Journal of Metamorphic Geology 8, 89-124.
9. Jochum, K. P.; Nohl, U.; Herwig, K.; Lammel, E.; Stoll, B.; Hofmann, A. W. 2005. GeoReM: A New Geochemical Database for Reference Materials and Isotopic Standards. Geostandards and Geoanalytical Research 29, 333-338.
10. Krogh Ravna, E. (2000). The garnet-clinopyroxene Fe^{2+}-Mg geothermometer: an updated calibration. Journal of Metamorphic Geology 18, 211-219.
11. Li, J.; John, T.; Gao, J.; Klemd, R.; Wang, X. 2017. Subduction channel fluid–rock interaction and mass transfer: Constraints from a retrograde vein in blueschist (SW Tianshan, China). Chemical Geology 456, 28-42.
12. Locatelli, M.; Verlaguet, A.; Agard, P.; Federico, L.; Angiboust, S. 2018. Intermediate-depth brecciation along the subduction plate interface (Monviso eclogite, W. Alps). Lithos 320, 378-402.
13. Penniston-Dorland, S. and Ferry, J. 2008. Element mobility and scale of mass transport in the formation of quartz veins during regional metamorphism of the Waits River Formation, east-central Vermont. American Mineralogist 93, 7–21.
14. Plümper, O.; John, T.; Podladchikov, Y.; Vrijmoed, J.; and Scambelluri, M. (2017). Fluid escape from subduction zones controlled by channel-forming reactive porosity. Nature Geoscience 10, 150-158.

15. Schmidt, M. and Poli, S. 1998. Experimentally based water budgets for dehydrating slabs and consequences for arc magma generation. Earth and Planetary Science Letters 163, 1–4, 361-379.
16. Spandler, C.; Pettke, T.; and Rubatto, D. (2011). Internal and external fluid sources for eclogite-facies veins in the Monviso meta-ophiolite, Western Alps: implications for fluid flow in subduction zones. Journal of Petrology 52, 1207-1236.
17. Spandler, C.; Pirard, C. 2013. Element recycling from subducting slabs to arc crust: A review. Lithos 170–17, 208-223.
18. van der Straaten, F.; Schenk, V.; John, T.; and Gao, J. (2008). Blueschist-facies rehydration of eclogites (Tian Shan, NW-China): Implications for fluid-rock interaction in the subduction channel. Chemical Geology 255, 1-2, 195-219.
19. Waters, D.J. and Martin, H.N. (1996). Geobarometry in phengite-bearing eclogites. Terra Abstracts 5, 410-411. DOI: https://www.earth.ox.ac.uk/~davewa/research/eclogites/ecbarcal.html
20. Whitney, D. 2016. "Classical" Thermobarometry. Integrating Research and Education, DOI: https://serc.carleton.edu/research_education/equilibria/classicalthermobarometry.html
21. "XRF and XRD Lab." Franklin & Marshall College, www.fandm.edu/earth-environment/laboratory-facilities/xrf-and-xrd-lab.

APPENDICES

Appendix 1: Raw wt% oxide data for garnet, omphacite, and phengite as well as uncertainty due to counting statistics.

Appendix 1a: Raw wt% oxide data for 5 host and 5 alteration garnets. The filter for accepted values is 1.5 wt% from 100 wt%. Values in green are accepted values.

Point No.	Na2O	FeO	TiO2	CaO	Al2O3	MgO	MnO	K2O	SiO2	Total	Comment
2	0.07	30.62	0.01	3.07	21.58	5.77	1.01	0.00	37.39	99.52	M17H820E01b Host 1 grt
3	0.06	30.44	0.02	3.61	21.50	5.45	1.11	0.01	37.64	99.85	M17H820E01b Host 1 grt
4	0.04	30.75	0.00	3.32	21.53	5.69	0.95	0.00	37.52	99.80	M17H820E01b Host 1 grt
5	0.04	30.68	0.05	2.77	21.44	5.77	1.27	0.01	37.50	99.53	M17H820E01b Host 1b grt
6	0.03	30.83	0.05	2.72	21.47	5.85	1.24	0.00	37.51	99.70	M17H820E01b Host 1b grt
7	0.03	30.81	0.05	2.57	21.45	5.90	1.37	0.00	37.53	99.71	M17H820E01b Host 1b grt
8	0.08	29.71	0.02	3.82	21.29	5.12	1.10	0.01	37.40	98.55	M17H820E01b Host 2 grt
9	0.05	29.30	0.04	3.96	21.27	4.93	1.85	0.00	37.24	98.64	M17H820E01b Host 2 grt
10	0.10	29.44	0.01	4.07	21.30	5.23	1.28	0.00	36.87	98.29	M17H820E01b Host 2 grt
11	0.06	30.50	0.04	4.24	21.33	4.84	1.14	0.00	37.16	99.31	M17H820E01b Host 3 grt
12	0.03	30.30	0.13	4.33	21.30	4.93	1.10	0.00	37.35	99.47	M17H820E01b Host 3 grt
13	0.07	30.56	0.12	3.98	21.40	5.02	1.13	0.02	37.43	99.72	M17H820E01b Host 3 grt
14	0.03	30.72	0.03	2.84	21.42	6.09	1.02	0.01	37.49	99.65	M17H820E01b Host 4 grt
15	0.03	30.15	0.13	3.18	21.35	5.72	0.98	0.02	37.28	98.83	M17H820E01b Host 4 grt
16	0.06	30.79	0.04	3.60	21.36	5.33	0.92	0.01	37.05	99.15	M17H820E01b Host 4 grt
17	0.03	29.93	0.02	3.57	21.50	6.15	0.69	0.02	37.68	99.59	M17H820E01b Alt 1 Grt
18	0.03	30.08	0.03	3.32	21.58	6.28	0.68	0.00	37.42	99.41	M17H820E01b Alt 1 Grt
19	0.02	29.36	0.00	3.01	21.45	6.29	0.71	0.02	37.42	98.27	M17H820E01b Alt 1 Grt
20	0.00	30.00	0.02	3.66	21.24	6.09	0.67	0.00	37.63	99.31	M17H820E01b Alt 2 grt
21	0.03	30.15	0.00	3.40	21.30	5.88	0.72	0.00	37.38	98.86	M17H820E01b Alt 2 grt
22	0.03	30.02	0.01	3.61	21.48	5.79	0.66	0.00	37.38	98.98	M17H820E01b Alt 2 grt
23	0.03	31.01	0.00	3.64	21.38	5.25	0.76	0.01	37.46	99.54	M17H820E01b Alt 3 grt
24	0.05	30.89	0.02	3.83	21.48	5.03	0.83	0.01	37.00	99.13	M17H820E01b Alt 3 grt
25	0.00	30.87	0.03	3.66	21.19	5.19	0.79	0.00	37.14	98.87	M17H820E01b Alt 3 grt
26	0.03	30.11	0.04	3.55	21.37	5.94	0.74	0.00	37.42	99.20	M17H820E01b Alt 4 grt
27	0.03	29.91	0.02	3.12	21.46	6.35	0.69	0.00	37.48	99.06	M17H820E01b Alt 4 grt
28	0.04	30.14	0.04	3.11	21.22	6.36	0.72	0.00	37.36	98.98	M17H820E01b Alt 4 grt
29	0.04	30.54	0.05	2.72	21.26	6.39	0.86	0.01	37.43	99.29	M17H820E01b Alt 5 grt
30	0.02	30.18	0.01	3.57	21.29	5.87	0.68	0.01	37.39	99.02	M17H820E01b Alt 5 grt
31	0.01	30.28	0.02	3.30	21.18	5.83	0.69	0.00	37.26	98.56	M17H820E01b Alt 5 grt

Appendix 1b: Raw wt% oxide data for 5 host and 5 alteration omphacites. The filter for accepted values is 1.5 wt% from 100 wt%. Values in green are accepted values, while those in red are unreasonable. Points 13-15 were replaced with points 56-60 near the bottom.

Point No.	Na2O	FeO	TiO2	CaO	Al2O3	MgO	MnO	K2O	SiO2	Total	Comment
2	10.98	5.78	0.06	5.52	16.37	3.79	0.02	0.01	56.47	99.00	M17H820E01b Host 1 omp
3	11.03	6.38	0.05	5.53	16.09	3.82	0.01	0.01	56.05	98.97	M17H820E01b Host 1 omp
4	12.62	8.39	0.09	2.41	17.23	1.86	0.13	0.01	56.01	98.75	M17H820E01b Host 1 omp
5	12.41	7.18	0.63	2.96	17.87	1.70	0.17	0.02	56.45	99.39	M17H820E01b Host 1b omp
6	9.70	5.66	0.06	8.13	14.35	5.56	0.04	0.00	55.78	99.29	M17H820E01b Host 1b omp
7	10.88	6.83	0.04	5.11	15.82	3.70	0.03	0.01	56.26	98.69	M17H820E01b Host 1b omp
8	12.37	10.44	0.12	2.80	15.55	1.98	0.13	0.01	55.56	98.95	M17H820E01b Host 1 omp inc
9	12.63	10.60	0.14	2.78	15.65	1.92	0.18	0.00	55.93	99.83	M17H820E01b Host 1 omp inc
10	9.95	8.33	0.06	7.29	13.23	4.85	0.05	0.00	55.79	99.56	M17H820E01b Host 1 omp
11	13.04	8.91	0.10	1.82	17.53	1.29	0.12	0.00	56.42	99.23	M17H820E01b Host 1 omp
12	11.81	7.93	0.06	4.06	15.87	2.90	0.02	0.00	55.60	98.25	M17H820E01b Host 1 omp
13	0.05	32.07	0.02	4.31	22.71	5.12	1.29	0.02	37.88	103.47	M17H820E01b Host 2 omp
14	0.05	32.32	0.01	4.08	22.65	4.96	1.26	0.00	37.86	103.19	M17H820E01b Host 2 omp
15	0.03	32.82	0.06	3.72	22.69	5.22	1.26	0.00	37.79	103.59	M17H820E01b Host 2 omp
16	5.41	23.40	0.18	3.17	19.13	3.66	1.73	0.03	43.13	99.84	M17H820E01b Host 2 omp
17	11.20	10.53	0.40	4.70	13.51	3.52	0.38	0.00	55.26	99.50	M17H820E01b Host 2 omp
18	11.66	9.95	0.05	4.38	14.21	3.11	0.10	0.03	55.70	99.18	M17H820E01b Host 3 omp
19	0.53	3.45	0.20	0.03	27.79	3.01	0.01	9.39	49.64	94.06	M17H820E01b Host 3 omp
20	12.72	10.28	0.07	2.15	16.43	1.39	0.10	0.01	56.07	99.22	M17H820E01b Host 3 omp
21	8.56	13.10	0.06	4.09	14.11	2.09	1.09	0.03	50.84	93.97	M17H820E01b Host 3 omp
22	12.27	9.38	0.22	2.95	15.86	2.09	0.19	0.01	55.38	98.35	M17H820E01b Host 3 omp
23	11.06	7.98	0.09	4.65	15.13	3.41	0.02	0.00	55.74	98.08	M17H820E01b Host 4 omp
24	10.16	8.06	0.09	6.20	14.00	4.37	0.07	0.01	55.26	98.22	M17H820E01b Host 4 omp
25	10.63	7.65	0.08	5.36	15.25	3.68	0.02	0.02	56.08	98.76	M17H820E01b Host 4 omp
26	10.39	6.96	0.10	6.25	15.04	4.22	0.05	0.01	56.33	99.35	M17H820E01b Host 4 omp
27	10.23	8.44	0.07	6.21	14.00	4.28	0.06	0.01	55.75	99.05	M17H820E01b Host 4 omp
28	12.47	9.55	0.06	2.45	16.51	1.71	0.14	0.02	56.11	99.02	M17H820E01b Host 4 omp inc
29	11.03	8.94	0.08	4.54	15.09	3.21	0.07	0.00	55.50	98.45	M17H820E01b Host 4 omp inc
30	7.61	8.17	0.03	11.16	9.49	7.52	0.12	0.00	54.96	99.06	M17H820E01b Alt 1 omp
31	8.51	10.70	0.07	8.17	11.20	5.55	0.10	0.52	53.76	98.58	M17H820E01b Alt 1 omp
32	8.34	8.03	0.02	10.41	10.22	6.82	0.05	0.02	54.52	98.43	M17H820E01b Alt 1 omp
33	8.52	8.33	0.04	9.88	10.68	6.51	0.08	0.03	55.31	99.38	M17H820E01b Alt 1 omp
34	7.97	8.47	0.00	10.75	9.61	7.07	0.07	0.00	54.99	98.93	M17H820E01b Alt 1 omp
35	11.09	8.46	0.03	5.26	14.74	3.58	0.08	0.00	55.97	99.21	M17H820E01b Alt 2 omp
36	10.40	8.57	0.05	6.16	13.49	4.47	0.04	0.01	55.17	98.36	M17H820E01b Alt 2 omp
37	11.56	7.92	0.05	4.43	16.13	3.09	0.07	0.00	56.19	99.44	M17H820E01b Alt 2 omp
38	11.31	7.82	0.05	4.93	15.45	3.45	0.04	0.02	55.59	98.66	M17H820E01b Alt 2 omp
39	11.08	7.93	0.06	5.23	15.36	3.68	0.03	0.00	55.77	99.14	M17H820E01b Alt 2 omp
40	9.69	8.74	0.03	7.65	12.16	5.25	0.05	0.01	55.43	99.01	M17H820E01b Alt 3 omp
41	12.05	6.95	0.02	3.78	17.29	2.73	0.08	0.02	56.50	99.41	M17H820E01b Alt 3 omp
42	11.15	8.26	0.06	5.16	14.93	3.66	0.04	0.00	56.05	99.30	M17H820E01b Alt 3 omp
43	11.58	7.41	0.08	3.95	16.53	2.85	0.06	0.15	56.10	98.70	M17H820E01b Alt 3 omp
44	11.63	8.21	0.35	4.07	15.63	3.14	0.10	0.00	55.88	99.01	M17H820E01b Alt 3 omp
45	8.97	8.09	0.17	9.15	11.61	6.02	0.06	0.01	55.50	99.57	M17H820E01b Alt 4 omp
46	12.22	7.60	0.09	3.32	17.41	2.40	0.07	0.00	56.32	99.43	M17H820E01b Alt 4 omp
47	10.15	8.38	0.07	7.26	13.12	4.95	0.06	0.00	55.58	99.56	M17H820E01b Alt 4 omp
48	10.40	9.00	0.07	6.48	13.17	4.58	0.05	0.00	55.71	99.47	M17H820E01b Alt 4 omp
49	12.56	5.55	0.08	2.65	19.50	1.99	0.04	0.00	56.96	99.33	M17H820E01b Alt 4 omp
50	10.04	5.59	0.05	7.13	15.30	4.82	0.04	0.00	56.31	99.27	M17H820E01b Alt 5 omp
51	11.99	6.05	0.05	3.59	18.38	2.49	0.04	0.00	56.76	99.36	M17H820E01b Alt 5 omp
52	12.63	7.68	0.19	1.96	17.79	2.24	0.07	0.02	56.57	99.16	M17H820E01b Alt 5 omp
53	11.87	7.15	0.10	3.91	16.94	2.75	0.07	0.02	56.79	99.59	M17H820E01b Alt 5 omp
54	11.62	7.53	0.09	4.36	16.13	3.10	0.02	0.00	56.15	99.01	M17H820E01b Alt 5 omp
55	11.21	7.89	0.08	3.88	16.87	3.39	0.05	0.40	55.52	99.28	M17H820E01b Alt 5 omp
56	12.34	13.23	0.56	2.71	12.79	1.72	0.22	0.02	55.46	99.05	M17H820E01b Host 2 omp
57	12.62	11.58	0.46	2.30	14.50	1.64	0.23	0.00	55.62	98.96	M17H820E01b Host 2 omp
58	10.76	8.42	0.08	5.85	13.93	3.93	0.11	0.00	55.93	99.01	M17H820E01b Host 2 omp
59	10.79	10.71	0.57	5.36	11.95	3.92	0.40	0.00	55.47	99.16	M17H820E01b Host 2 omp
60	12.63	10.62	0.40	2.13	15.11	1.81	0.17	0.00	55.95	98.82	M17H820E01b Host 2 omp

Appendix 1c: Raw wt% oxide data for 5 host and 5 alteration phengites. The filter for accepted values is 1.5 wt% from 95 wt%. Values in green are accepted values, while those in red are unreasonable.

Point No.	Na2O	FeO	TiO2	CaO	Al2O3	MgO	MnO	K2O	SiO2	Total	Comment
2	0.02	2.97	0.12	0.02	20.63	5.37	0.01	10.75	54.08	93.97	M17H820E01b Host 1 phg
3	0.02	2.92	0.12	0.00	20.61	5.37	0.01	10.74	53.75	93.54	M17H820E01b Host 1 phg
4	0.04	2.83	0.07	0.00	20.68	5.41	0.05	10.75	54.37	94.19	M17H820E01b Host 1 phg
5	0.07	3.34	0.11	0.01	20.88	5.68	0.03	10.75	53.94	94.81	M17H820E01b Host 1b phg
6	0.02	3.29	0.15	0.00	19.46	5.89	0.00	11.08	55.00	94.89	M17H820E01b Host 1b phg
7	0.05	2.79	0.08	0.01	18.70	6.19	0.00	10.83	55.21	93.86	M17H820E01b Host 1b phg
8	0.18	3.00	0.11	0.00	24.02	4.10	0.01	10.90	52.03	94.35	M17H820E01b Host 2 phg
9	0.12	3.33	0.12	0.00	23.77	4.27	0.06	10.83	51.67	94.17	M17H820E01b Host 2 phg
10	0.20	3.28	0.14	0.02	25.32	3.73	0.02	10.88	51.92	95.51	M17H820E01b Host 2 phg
11	0.12	3.25	0.19	0.03	23.66	4.10	0.05	10.80	52.06	94.25	M17H820E01b Host 3 phg
12	0.09	3.11	0.18	0.01	23.49	4.22	0.02	10.70	51.10	92.92	M17H820E01b Host 3 phg
13	0.32	3.33	0.10	0.02	26.41	3.34	0.04	10.58	51.27	95.40	M17H820E01b Host 3 phg
14	0.12	3.50	0.11	0.00	21.78	4.74	0.00	10.47	53.23	93.95	M17H820E01b Host 4 phg
15	0.09	3.47	0.11	0.01	22.01	4.79	0.00	10.66	52.20	93.35	M17H820E01b Host 4 phg
16	0.10	3.69	0.16	0.02	21.65	4.86	0.05	10.59	53.00	94.12	M17H820E01b Host 4 phg
17	0.07	3.01	0.14	0.00	22.13	5.01	0.02	10.71	53.06	94.14	M17H820E01b Alt 1 phg
18	0.07	2.86	0.20	0.00	21.60	5.15	0.00	10.60	52.80	93.28	M17H820E01b Alt 1 phg
19	0.08	2.90	0.17	0.01	22.21	4.98	0.00	10.76	52.41	93.52	M17H820E01b Alt 1 phg
20	0.03	2.99	0.14	0.00	21.34	5.41	0.00	10.96	54.28	95.15	M17H820E01b Alt 2 phg
21	0.02	2.91	0.09	0.03	20.80	5.13	0.02	10.63	53.06	92.70	M17H820E01b Alt 2 phg
22	0.09	2.97	0.07	0.00	20.76	5.07	0.02	10.73	53.72	93.43	M17H820E01b Alt 2 phg
23	0.07	3.26	0.14	0.00	20.66	4.84	0.00	10.46	51.85	91.27	M17H820E01b Alt 3 phg
24	0.06	3.02	0.13	0.00	22.12	4.82	0.01	10.73	53.26	94.16	M17H820E01b Alt 3 phg
25	0.08	3.16	0.12	0.00	22.35	4.67	0.00	10.74	52.77	93.89	M17H820E01b Alt 3 phg
26	0.05	2.76	0.11	0.03	21.68	5.24	0.00	11.05	53.31	94.23	M17H820E01b Alt 4 phg
27	11.79	5.85	0.08	3.73	17.29	2.55	0.02	0.02	56.95	98.27	M17H820E01b Alt 4 phg
28	2.31	3.45	0.18	0.66	22.72	3.58	0.00	8.62	51.85	93.36	M17H820E01b Alt 4 phg
29	9.55	5.04	0.01	8.22	14.00	5.48	0.04	0.00	56.76	99.11	M17H820E01b Alt 5 phg
30	11.20	6.43	0.04	4.73	15.75	3.23	0.04	0.00	56.95	98.38	M17H820E01b Alt 5 phg
31	6.83	10.18	0.00	0.72	9.00	11.60	0.04	0.12	57.43	95.91	M17H820E01b Alt 5 phg
32	0.02	2.61	0.14	0.00	20.86	5.38	0.00	10.72	54.25	93.98	27 Redo M17H820E01b Alt 4 phg

Appendix 1d: Table of relative uncertainties (1σ) due to counting statistics on the microprobe for each major element of each garnet point.

	Na	Fe	Ti	Ca	Al	Mg	Mn	K	Si
2	18.09	0.37	>100	1.05	0.34	0.74	2.71	100.00	0.36
3	20.99	0.37	93.87	0.97	0.34	0.77	2.47	97.15	0.36
4	34.86	0.37	100.00	1.02	0.34	0.75	2.72	>100	0.36
5	35.68	0.37	37.26	1.13	0.34	0.74	2.25	>100	0.36
6	49.74	0.37	37.96	1.14	0.34	0.74	2.32	100.00	0.36
7	51.31	0.37	39.41	1.17	0.34	0.73	2.13	100.00	0.36
8	18.91	0.38	94.05	0.94	0.34	0.79	2.49	70.93	0.36
9	30.47	0.38	46.71	0.93	0.34	0.81	1.79	100.00	0.36
10	14.94	0.38	>100	0.91	0.34	0.78	2.24	>100	0.37
11	22.25	0.37	58.71	0.89	0.34	0.82	2.46	100.00	0.36
12	44.35	0.38	15.28	0.88	0.34	0.81	2.48	100.00	0.36
13	21.05	0.37	17.47	0.93	0.34	0.80	2.44	46.32	0.36
14	48.66	0.37	58.18	1.12	0.34	0.72	2.58	>100	0.36
15	51.69	0.38	15.51	1.04	0.34	0.74	2.70	52.07	0.36
16	22.91	0.37	51.43	0.97	0.34	0.77	2.81	>100	0.36
17	44.35	0.38	92.06	0.98	0.34	0.72	3.45	52.37	0.36
18	53.76	0.38	79.72	1.02	0.34	0.71	3.56	100.00	0.36
19	71.31	0.38	100.00	1.08	0.34	0.71	3.30	47.54	0.36
20	>100	0.38	>100	0.96	0.34	0.72	3.50	100.00	0.36
21	50.52	0.38	100.00	1.01	0.34	0.74	3.33	100.00	0.36
22	39.99	0.38	>100	0.97	0.34	0.74	3.51	>100	0.36
23	54.84	0.37	100.00	0.97	0.34	0.78	3.20	>100	0.36
24	30.62	0.37	>100	0.93	0.34	0.80	2.99	77.38	0.36
25	>100	0.37	70.85	0.96	0.34	0.79	3.15	>100	0.36
26	42.82	0.38	50.51	0.98	0.34	0.73	3.25	>100	0.36
27	47.43	0.38	>100	1.06	0.34	0.71	3.49	>100	0.36
28	35.28	0.38	50.79	1.06	0.34	0.70	3.38	100.00	0.36
29	36.81	0.37	42.54	1.14	0.34	0.70	2.92	90.15	0.36
30	63.74	0.38	>100	0.98	0.34	0.73	3.53	>100	0.36
31	>100	0.37	>100	1.02	0.34	0.74	3.45	100.00	0.36

Appendix 1e: Table of relative uncertainties (1σ) due to counting statistics on the microprobe for each major element of each omphacite point.

	Na	Fe	Ti	Ca	Al	Mg	Mn	K	Si
2	0.69	1.06	34.19	0.85	0.43	0.96	>100	>100	0.32
3	0.69	1.01	39.80	0.85	0.44	0.96	>100	>100	0.32
4	0.64	0.87	23.33	1.33	0.42	1.46	14.09	87.71	0.32
5	0.65	0.94	4.02	1.19	0.42	1.52	10.96	46.82	0.32
6	0.73	1.08	35.28	0.69	0.47	0.79	39.36	>100	0.32
7	0.69	0.97	51.30	0.88	0.44	0.98	58.25	58.79	0.32
8	0.66	0.77	19.63	1.22	0.45	1.41	14.75	>100	0.32
9	0.65	0.77	16.20	1.22	0.45	1.43	10.42	>100	0.32
10	0.74	0.87	33.52	0.73	0.49	0.85	34.00	100.00	0.32
11	0.64	0.84	21.55	1.56	0.42	1.80	15.64	100.00	0.32
12	0.67	0.90	32.80	1.00	0.44	1.13	>100	100.00	0.32
13	35.21	0.43	>100	0.96	0.38	0.87	2.47	46.39	0.40
14	34.47	0.43	>100	0.99	0.38	0.89	2.49	100.00	0.40
15	51.46	0.42	36.70	1.05	0.38	0.87	2.50	100.00	0.41
16	1.10	0.51	12.18	1.14	0.41	1.04	2.03	31.71	0.38
17	0.70	0.77	5.99	0.92	0.49	1.03	5.93	100.00	0.32
18	0.68	0.79	42.17	0.96	0.47	1.09	19.35	33.71	0.32
19	3.70	1.43	11.41	37.48	0.32	1.05	>100	0.59	0.34
20	0.65	0.78	32.61	1.41	0.44	1.74	17.27	>100	0.32
21	0.82	0.69	35.13	0.99	0.48	1.36	2.68	28.18	0.34
22	0.66	0.82	10.79	1.19	0.44	1.35	10.10	>100	0.32
23	0.69	0.89	24.40	0.93	0.46	1.03	85.11	>100	0.32
24	0.73	0.89	24.42	0.80	0.47	0.90	23.58	86.07	0.32
25	0.70	0.91	28.24	0.86	0.45	0.99	82.25	42.26	0.32
26	0.71	0.96	19.89	0.80	0.45	0.91	36.36	>100	0.32
27	0.72	0.87	30.27	0.80	0.47	0.91	31.10	>100	0.32
28	0.65	0.81	39.01	1.32	0.44	1.53	12.85	30.55	0.32
29	0.70	0.84	28.85	0.94	0.46	1.07	26.03	>100	0.32
30	0.85	0.88	66.83	0.59	0.58	0.67	14.40	>100	0.32
31	0.81	0.77	28.85	0.69	0.54	0.80	18.75	2.88	0.33
32	0.81	0.89	>100	0.61	0.56	0.71	33.80	41.57	0.32
33	0.80	0.87	49.93	0.63	0.55	0.73	22.98	29.15	0.32
34	0.83	0.86	>100	0.60	0.58	0.70	28.96	100.00	0.32
35	0.69	0.87	66.38	0.87	0.46	1.00	22.12	100.00	0.32
36	0.72	0.86	45.56	0.80	0.48	0.89	47.97	59.58	0.32
37	0.67	0.89	45.94	0.95	0.44	1.08	25.49	100.00	0.32
38	0.68	0.90	38.97	0.90	0.45	1.04	40.82	47.09	0.32
39	0.69	0.90	34.47	0.88	0.45	0.99	59.89	100.00	0.32
40	0.75	0.85	85.51	0.71	0.51	0.82	36.33	70.42	0.32
41	0.66	0.96	>100	1.04	0.42	1.16	21.24	50.00	0.32
42	0.69	0.88	38.47	0.88	0.46	0.99	45.81	>100	0.32
43	0.67	0.93	27.42	1.02	0.43	1.14	30.66	6.84	0.32
44	0.68	0.88	6.52	0.99	0.45	1.08	18.33	100.00	0.32
45	0.78	0.89	13.92	0.65	0.52	0.76	33.55	73.71	0.32
46	0.65	0.92	26.69	1.12	0.42	1.25	24.03	>100	0.32
47	0.73	0.87	31.46	0.73	0.49	0.84	30.82	100.00	0.32
48	0.72	0.84	30.93	0.78	0.49	0.88	33.56	>100	0.32
49	0.63	1.09	26.62	1.26	0.39	1.38	43.59	>100	0.32
50	0.72	1.09	49.12	0.74	0.45	0.85	43.70	100.00	0.32
51	0.65	1.04	39.83	1.07	0.41	1.21	38.55	>100	0.32
52	0.64	0.92	11.43	1.51	0.42	1.30	23.92	46.70	0.32
53	0.66	0.95	21.42	1.02	0.43	1.16	25.89	37.39	0.32
54	0.67	0.92	23.05	0.96	0.44	1.09	83.67	100.00	0.32
55	0.68	0.90	27.78	1.02	0.43	1.03	37.51	3.37	0.32
56	0.68	0.67	4.43	1.24	0.5	1.54	9.04	48.01	0.32
57	0.66	0.71	5.34	1.36	0.47	1.57	8.9	100	0.32
58	0.71	0.85	28.76	0.82	0.47	0.96	16.12	>100	0.32
59	0.72	0.75	4.55	0.86	0.52	0.97	5.67	>100	0.32
60	0.66	0.75	6.05	1.42	0.46	1.49	11.72	100	0.32

Appendix 1f: Table of relative uncertainties (1σ) due to counting statistics on the microprobe for each major element of each phengite point.

	Na	Fe	Ti	Ca	Al	Mg	Mn	K	Si
2	86.64	2.16	24.47	0.81	0.53	1.10	>100	>100	0.47
3	69.50	2.16	25.08	0.80	0.53	1.08	>100	100.00	0.47
4	39.26	2.19	47.56	0.81	0.53	1.09	50.84	100.00	0.47
5	25.31	1.98	30.01	0.80	0.53	1.06	83.23	>100	0.47
6	72.73	2.01	21.28	0.80	0.55	1.04	100.00	100.00	0.47
7	30.76	2.23	39.45	0.80	0.56	1.01	100.00	>100	0.46
8	10.49	2.08	28.54	0.80	0.49	1.26	>100	>100	0.48
9	15.71	1.97	27.00	0.80	0.49	1.23	40.98	100.00	0.48
10	11.19	2.00	22.94	0.81	0.48	1.34	>100	96.21	0.48
11	16.40	1.99	17.12	0.80	0.49	1.26	50.82	58.13	0.48
12	18.66	2.05	16.57	0.81	0.49	1.23	95.83	>100	0.48
13	7.86	2.00	33.46	0.82	0.47	1.42	68.61	68.31	0.49
14	15.17	1.93	29.01	0.82	0.51	1.16	100.00	>100	0.47
15	19.08	1.93	30.05	0.81	0.51	1.16	100.00	>100	0.48
16	18.24	1.86	20.55	0.81	0.51	1.15	40.98	96.21	0.47
17	25.51	2.14	23.87	0.81	0.51	1.12	>100	100.00	0.47
18	22.30	2.13	15.94	0.81	0.52	1.11	100.00	100.00	0.47
19	19.05	2.13	17.41	0.81	0.51	1.13	100.00	>100	0.48
20	47.24	2.13	22.94	0.80	0.52	1.08	100.00	100.00	0.47
21	73.60	2.12	36.71	0.81	0.53	1.11	>100	51.70	0.47
22	19.20	2.11	42.81	0.81	0.53	1.12	>100	100.00	0.47
23	26.33	2.02	22.94	0.82	0.53	1.15	100.00	100.00	0.48
24	29.15	2.14	23.87	0.81	0.51	1.15	>100	100.00	0.47
25	19.69	2.06	27.33	0.81	0.51	1.16	100.00	>100	0.48
26	34.33	2.19	31.04	0.80	0.51	1.10	>100	46.29	0.47
27	0.94	1.44	36.74	73.42	0.59	1.70	>100	1.51	0.46
28	2.22	1.96	17.27	0.90	0.50	1.36	>100	4.22	0.48
29	1.05	1.56	226.24	100.00	0.66	1.12	59.09	0.99	0.46
30	0.97	1.38	70.71	100.00	0.62	1.51	57.05	1.33	0.46
31	1.28	1.08	100.00	11.17	0.85	0.76	76.27	3.91	0.46
32	76.93	2.28	22.78	0.81	0.53	1.08	100.00	100.00	0.47

Appendix 2: Cation values calculated for garnet, omphacite, and phengite.

Appendix 2.1: Cation values calculated for garnet using wt% oxide values from the microprobe normalized to 12 O.

No.	Na	Fe	Ti	Ca	Al	Mg	Mn	K	Si
2	0.01	2.03	0.00	0.26	2.02	0.68	0.07	0.00	2.96
3	0.00	2.01	0.00	0.31	2.00	0.64	0.07	0.00	2.98
4	0.00	2.03	0.00	0.28	2.01	0.67	0.06	0.00	2.97
5	0.00	2.03	0.00	0.24	2.00	0.68	0.09	0.00	2.97
6	0.00	2.04	0.00	0.23	2.00	0.69	0.08	0.00	2.97
7	0.00	2.04	0.00	0.22	2.00	0.70	0.09	0.00	2.97
8	0.01	1.99	0.00	0.33	2.01	0.61	0.07	0.00	2.99
9	0.00	1.96	0.00	0.34	2.01	0.59	0.13	0.00	2.98
10	0.01	1.98	0.00	0.35	2.02	0.63	0.09	0.00	2.96
11	0.00	2.04	0.00	0.36	2.01	0.58	0.08	0.00	2.97
12	0.00	2.02	0.01	0.37	2.00	0.58	0.07	0.00	2.97
13	0.01	2.03	0.01	0.34	2.00	0.59	0.08	0.00	2.97
14	0.00	2.03	0.00	0.24	2.00	0.72	0.07	0.00	2.97
15	0.00	2.01	0.01	0.27	2.01	0.68	0.07	0.00	2.97
16	0.00	2.06	0.00	0.31	2.01	0.63	0.06	0.00	2.96
17	0.00	1.98	0.00	0.30	2.00	0.72	0.05	0.00	2.97
18	0.00	1.99	0.00	0.28	2.01	0.74	0.05	0.00	2.96
19	0.00	1.96	0.00	0.26	2.02	0.75	0.05	0.00	2.98
20	0.00	1.99	0.00	0.31	1.98	0.72	0.04	0.00	2.98
21	0.00	2.01	0.00	0.29	2.00	0.70	0.05	0.00	2.98
22	0.00	2.00	0.00	0.31	2.01	0.69	0.04	0.00	2.97
23	0.00	2.06	0.00	0.31	2.00	0.62	0.05	0.00	2.98
24	0.00	2.06	0.00	0.33	2.02	0.60	0.06	0.00	2.96
25	0.00	2.07	0.00	0.31	2.00	0.62	0.05	0.00	2.97
26	0.00	2.00	0.00	0.30	2.00	0.70	0.05	0.00	2.97
27	0.00	1.98	0.00	0.27	2.01	0.75	0.05	0.00	2.97
28	0.00	2.00	0.00	0.26	1.99	0.75	0.05	0.00	2.97
29	0.00	2.03	0.00	0.23	1.99	0.76	0.06	0.00	2.97
30	0.00	2.01	0.00	0.30	2.00	0.70	0.05	0.00	2.97
31	0.00	2.02	0.00	0.28	2.00	0.69	0.05	0.00	2.98

Appendix 2.2: Cation values calculated for omphacite using wt% oxide values from the microprobe normalized to 6 O.

No.	Na	Fe	Ti	Ca	Al	Mg	Mn	K	Si
2	0.75560784	0.17157168	0.00168224	0.20992273	0.68478953	0.20053723	0.00048099	0.0004528	2.00445414
3	0.76242223	0.19022358	0.00144832	0.21123771	0.67606803	0.20302293	0.00030196	0.00045481	1.9983883
4	0.87728913	0.25157588	0.00242761	0.09258203	0.72808652	0.0994164	0.00394775	0.00041166	2.00832128
5	0.85247128	0.21274339	0.01689855	0.11236368	0.74618557	0.08978806	0.00519131	0.00072317	2.00012044
6	0.67086179	0.16885013	0.00166382	0.3107264	0.60329197	0.29566356	0.00132934	0	1.98986704
7	0.75408724	0.20419121	0.00115641	0.1957221	0.66652047	0.19717693	0.00087804	0.00059285	2.01129906
8	0.86908808	0.31638671	0.00313505	0.10871223	0.66410814	0.1069599	0.00383643	0.00046228	2.01344863
9	0.88062996	0.31880095	0.00367944	0.10711769	0.66331339	0.10293262	0.00551305	0	2.01149588
10	0.6940729	0.25064016	0.0017052	0.28101909	0.56099136	0.260127	0.00158456	0	2.00734766
11	0.90266982	0.26604352	0.00279342	0.0696224	0.73764528	0.06839371	0.00353802	0	2.01450634
12	0.82699355	0.23952401	0.00173894	0.15711026	0.67552818	0.15613919	0.00052002	0	2.00821979
13	0.00335215	1.03046682	0.0006359	0.17742506	1.02835452	0.2932534	0.04197823	0.00088226	1.45547786
14	0.00358651	1.04165952	0.0003769	0.16846793	1.02875822	0.28495361	0.04096354	0	1.45913551
15	0.00253375	1.05498621	0.00170604	0.15319824	1.0278586	0.29910023	0.04105089	0	1.45259879
16	0.40470132	0.75505199	0.00534081	0.13104574	0.86989461	0.21051358	0.05653357	0.00123052	1.66418283
17	0.7882953	0.31968549	0.01097866	0.18280794	0.57801696	0.19049135	0.01156064	0	2.00616209
18	0.81879142	0.30138488	0.00147137	0.16997112	0.60657308	0.16791783	0.00294489	0.00115512	2.01750284
19	0.03819558	0.10644238	0.00552303	0.00118582	1.20829983	0.16553889	0.00043744	0.44192556	1.83141955
20	0.88770569	0.30945582	0.00184138	0.08291758	0.6970016	0.07453252	0.00317058	0.00036735	2.01835091
21	0.64488961	0.42570285	0.00178317	0.17027904	0.64617916	0.12106527	0.0357079	0.00148711	1.97561075
22	0.86344199	0.28471811	0.00587056	0.11471941	0.67843165	0.11308281	0.00593293	0.00032411	2.01013756
23	0.77577549	0.24143902	0.00244949	0.18024373	0.64511059	0.18390646	0.00064346	0	2.01665736
24	0.71533803	0.24478021	0.0024041	0.24123237	0.59918366	0.23657058	0.002276	0.00041694	2.00683984
25	0.73958365	0.22958268	0.00202473	0.20608439	0.64496804	0.19686275	0.00066865	0.00082402	2.01254808
26	0.71800616	0.20746532	0.00276186	0.23868159	0.63179296	0.22422641	0.00147922	0.00036376	2.00787467
27	0.7150476	0.25446345	0.00197986	0.2398707	0.59484207	0.23001957	0.00174043	0.00045991	2.00996464
28	0.86925728	0.28715005	0.00151468	0.09437876	0.69958949	0.09165152	0.00429362	0.00110079	2.01746671
29	0.7744919	0.27077124	0.00204341	0.17616657	0.64408758	0.1733038	0.0020858	0	2.01010422
30	0.53903662	0.24961996	0.0008795	0.4368417	0.40861485	0.40955586	0.003775	0	2.00800395
31	0.61080161	0.33126689	0.00206089	0.32405517	0.48865568	0.30628469	0.0030727	0.02451036	1.99027963
32	0.59404838	0.24671466	0.00049749	0.40976303	0.44250785	0.37350965	0.00164913	0.00089047	2.00306867
33	0.60006673	0.25306297	0.00114779	0.38454147	0.45724138	0.35253532	0.00236905	0.00134391	2.00931412
34	0.56568862	0.25931413	0	0.42165171	0.41462628	0.38583376	0.00201537	0	2.01320066
35	0.77289362	0.25432098	0.00086535	0.20258169	0.62445332	0.19183723	0.00240513	0	2.01199875
36	0.73404262	0.26091101	0.00128718	0.24026744	0.57878092	0.24258121	0.00114081	0.00060373	2.00851531
37	0.79944356	0.2362538	0.00126119	0.16930118	0.67807644	0.16430476	0.0020845	0	2.00434847
38	0.78993326	0.23559073	0.00146344	0.19028344	0.65594979	0.18527148	0.00131196	0.00078125	2.00266679
39	0.77051487	0.23786914	0.00169994	0.20098758	0.64930208	0.19676632	0.00088097	0	2.00044277
40	0.68244995	0.26551075	0.00068319	0.29773833	0.52058892	0.28429421	0.00147676	0.00055608	2.01361359
41	0.82804564	0.20600401	0.00045328	0.14354409	0.72223169	0.14424194	0.00234145	0.00067822	2.00262624
42	0.77522302	0.24771681	0.00148377	0.19825666	0.630995	0.19565663	0.00115414	0	2.0100721
43	0.8037979	0.22186059	0.00212774	0.15151711	0.69746992	0.15210548	0.00169805	0.00666811	2.00856271
44	0.80920151	0.24640174	0.00950324	0.15649399	0.66107429	0.16798415	0.0029483	0	2.00547657
45	0.62832911	0.24443698	0.00448467	0.35419474	0.49435767	0.32422979	0.00168299	0.00050699	2.0052658
46	0.84140071	0.22571941	0.00227093	0.12632696	0.72869327	0.12705876	0.00216564	0	2.00022356
47	0.70909674	0.25252659	0.0017891	0.28028661	0.55716984	0.26589265	0.00177007	0	2.00282137
48	0.72775635	0.2716557	0.00195496	0.25058435	0.56021245	0.2464222	0.00162014	0	2.01080542
49	0.85357593	0.16269311	0.00210957	0.09952328	0.8055666	0.10398418	0.00109844	0	1.99667199
50	0.69106776	0.16596724	0.00120185	0.27120815	0.6401661	0.2550913	0.0011426	0	1.99920199
51	0.81865991	0.17818181	0.00137765	0.13545813	0.76285881	0.130721	0.00128255	0	1.99899152
52	0.86902898	0.2279375	0.00517946	0.07452693	0.74408264	0.11850607	0.00222426	0.00076965	2.00771152
53	0.8145415	0.21163729	0.00255615	0.14827418	0.70662699	0.14509648	0.00200845	0.00090303	2.01010428
54	0.80539884	0.22512488	0.00252805	0.16700045	0.6796003	0.16520693	0.00066612	0	2.00742283
55	0.77643956	0.2357234	0.00201565	0.14851149	0.71028304	0.18053584	0.00145233	0.01813831	1.98351608

Appendix 2.3: Cation values calculated for phengite using wt% oxide values from the microprobe normalized to 11 O.

No.	Na	Fe	Ti	Ca	Al	Mg	Mn	K	Si
2	0.002629	0.168428	0.006326	0.001308	1.648727	0.542839	0.000632	0.929941	3.667382
3	0.002774	0.166381	0.006253	0	1.654967	0.545423	0.000404	0.933497	3.66235
4	0.004979	0.159942	0.003406	0	1.647091	0.545019	0.002747	0.926772	3.674483
5	0.00941	0.188294	0.005426	0.000578	1.658869	0.570791	0.001599	0.924459	3.636323
6	0.003005	0.185389	0.007603	0	1.54533	0.591617	0	0.952391	3.706047
7	0.006314	0.158305	0.004083	0.000654	1.495285	0.626067	0	0.937364	3.74602
8	0.02363	0.16988	0.005756	0	1.916831	0.413849	0.000573	0.941531	3.523179
9	0.015557	0.189365	0.00619	0	1.904909	0.432833	0.00334	0.939444	3.513609
10	0.025833	0.183664	0.006901	0.001291	1.998042	0.372303	0.001248	0.929324	3.476526
11	0.015521	0.184394	0.009595	0.002035	1.891775	0.414654	0.002816	0.934708	3.532067
12	0.012276	0.178997	0.009164	0.000737	1.905276	0.432947	0.001341	0.939412	3.516946
13	0.041029	0.186499	0.004937	0.001722	2.084449	0.333439	0.002042	0.90387	3.43365
14	0.016332	0.198841	0.005622	0	1.743756	0.480014	0	0.907344	3.616215
15	0.012496	0.198978	0.005726	0.000808	1.778632	0.489609	0	0.932439	3.579369
16	0.013184	0.209851	0.007981	0.001239	1.735132	0.492672	0.003053	0.918688	3.604295
17	0.00867	0.170552	0.007085	0	1.767107	0.506019	0.00109	0.925696	3.595163
18	0.009803	0.163425	0.010178	0	1.739393	0.524564	0	0.923947	3.607845
19	0.010985	0.165549	0.00873	0.000731	1.786764	0.506752	0	0.936976	3.577691
20	0.004419	0.16763	0.006909	0	1.686033	0.54065	0	0.937302	3.638995
21	0.0032	0.167346	0.004656	0.00221	1.685686	0.52587	0.001281	0.93249	3.648804
22	0.011772	0.169445	0.003746	0	1.669133	0.515607	0.00104	0.933814	3.664961
23	0.009095	0.190883	0.007111	0	1.704788	0.505164	0	0.934263	3.630435
24	0.008008	0.171016	0.006622	0	1.765247	0.486536	0.000803	0.926867	3.606546
25	0.010811	0.179701	0.005985	0	1.791151	0.47339	0	0.931657	3.588489
26	0.006568	0.156379	0.005352	0.002395	1.731091	0.529224	0	0.955037	3.611929
27	1.490161	0.318933	0.003972	0.260528	1.328399	0.247811	0.000828	0.001497	3.712764
28	0.306383	0.197377	0.009058	0.048009	1.831789	0.365088	0	0.752267	3.547201
29	1.206716	0.274698	0.000686	0.573984	1.075336	0.532407	0.002429	0	3.699374
30	1.422052	0.352154	0.002168	0.331883	1.215605	0.315327	0.00244	0	3.729713
31	0.887769	0.570756	0	0.051358	0.711109	1.159309	0.001987	0.010605	3.850369
32	0.002753	0.147615	0.007123	0	1.662622	0.542386	0	0.92485	3.66901

Appendix 3: Bulk rock chemistry raw data.

Appendix 3.1: Major element raw data from XRF analysis at Franklin and Marshall College.

Specimen	E01-1	E01-2	E01-3	E01-4	E01-5	E01-6	E01-7	E01-8	E01-9	E01-10
SiO2	53.96	52.69	52.60	51.38	50.98	53.67	54.83	53.04	54.58	52.81
TiO2	1.04	1.73	2.00	2.27	2.01	1.52	1.16	1.13	1.02	0.43
Al2O3	16.39	16.49	15.69	15.14	15.52	14.99	14.78	15.37	15.99	14.60
Fe2O3T	9.41	10.70	10.70	11.98	12.07	9.72	9.06	11.68	9.44	7.15
MnO	0.12	0.19	0.18	0.24	0.24	0.11	0.07	0.14	0.09	0.05
MgO	2.09	2.19	2.29	2.44	2.84	4.29	5.54	5.68	5.76	4.02
CaO	3.16	3.59	3.98	4.33	4.63	4.34	3.86	3.65	3.01	7.99
Na2O	13.42	11.62	11.79	11.07	10.57	10.52	9.99	8.53	8.48	9.40
K2O	0.13	0.16	0.10	0.10	0.15	0.26	0.31	0.61	1.35	0.68
P2O5	0.16	0.48	0.66	0.80	0.75	0.41	0.26	0.15	0.11	2.66
Total	**99.88**	**99.84**	**99.99**	**99.75**	**99.76**	**99.83**	**99.86**	**99.98**	**99.83**	**99.79**
LOI	-0.88	2.80	0.48	0.29	0.29	0.37	1.06	0.69	1.41	-1.25

Appendix 3.2: Processed trace element data collected from the Element-2 ICP-MS. 1-5 are the host; 6-9 are the alteration. 10 is the vein.

	Sample	TH1	TH2	TH3	TH4	TH5	TH6	TH7	TH8	TH9	TH10
	Rank	1	2	3	4	5	6	7	8	9	10
Element		ppm	ppm	ppm	ppm	ppm	ppm	ppm	ppm	ppm	ppm
Fe	1	91273.72	105297.7	108564.2	116335.4	116154.5	94863.9	82395.37	111854.5	94850.41	73217.91
Ti	2	9517.285	13648.12	18834.22	20375.8	19146.81	14672.73	10831.46	11202.95	10235.3	5254.199
Fe/1e4	1	9.127372	10.52977	10.85642	11.63354	11.61545	9.48639	8.239537	11.18545	9.485041	7.321791
Ti/1e4	2	0.951729	1.364812	1.883422	2.03758	1.914681	1.467273	1.083146	1.120295	1.02353	0.52542
Li	3	25.7227	25.49379	23.67937	24.04558	24.00505	25.00519	22.63252	22.34627	29.59333	20.28078
Sc	4	19.90477	27.17306	27.6726	27.94503	27.7257	29.09086	26.45334	32.14577	29.16464	25.38667
V	5	103.1888	148.1171	174.6423	205.3136	210.2196	252.5884	220.1422	206.4242	235.0102	212.9464
Cr	6	135.8671	163.9066	159.5404	165.5217	176.1791	244.5363	277.9096	304.5181	289.549	259.5004
Ni	7	88.14183	102.3517	94.85719	107.2409	96.98283	116.8241	124.4998	400.2651	119.3313	105.0055
Cu	8	66.23811	116.5032	151.5572	109.2471	74.36009	90.82751	66.37677	281.8828	81.11275	79.42845
Zn	9	91.78654	132.5153	129.5768	163.9886	201.7011	111.9932	130.4175	122.3165	125.0719	112.0992
Rb	10	4.26713	5.584171	4.946345	5.862391	5.183049	5.442765	6.381863	7.982363	14.92705	12.06438
Sr	11	47.45056	85.30152	94.35156	187.0478	170.9319	73.60518	61.13942	63.41042	62.86764	227.5457
Y	12	52.23343	101.3774	96.18814	139.3478	136.556	52.43203	27.59582	49.24544	25.19651	89.66222
Zr	13	37.20002	39.54834	41.07359	35.20656	37.15998	29.21084	25.49418	25.70108	25.06585	18.14315
Nb	14	6.088362	9.082947	13.83957	13.14888	11.01933	8.086614	4.759768	4.551738	4.021516	2.98548
Mo	15	4.102063	4.498758	5.447645	5.716729	5.83524	7.606035	4.283882	5.296035	6.228108	4.498485
Cs	16	0.053991	0.073914	0.064166	0.125772	0.103808	0.089779	0.104693	0.11541	0.19157	0.139585
Ba	17	87.30394	133.8774	124.016	121.3359	216.8079	117.0798	109.475	108.8135	124.2058	121.3451
La	18	26.53109	14.97711	16.94866	21.70725	20.90861	9.486447	4.638001	2.879983	2.330396	23.3551
Ce	19	83.76572	48.18141	57.24464	69.99381	66.26873	30.96618	15.66845	9.530051	6.271137	66.10674
Pr	20	13.49292	8.078499	9.331017	11.52723	11.01283	5.031896	2.395371	1.512969	0.807724	10.31373
Nd	21	62.54169	39.02555	45.5186	55.30728	54.2253	25.01126	12.53143	8.291357	3.818838	53.5537
Sm	22	14.61868	10.36372	12.55337	15.05547	14.39048	7.704639	4.619295	3.49095	2.12366	19.11806
Eu	23	3.568325	2.990678	3.575484	4.449903	4.302977	2.395463	1.507194	1.174857	0.718153	7.564995
Gd	24	12.02301	10.16025	11.60289	14.63732	14.69477	7.399744	4.142267	3.282361	1.778826	20.24915
Tb	25	1.668272	2.132464	2.376681	3.161016	3.32669	1.724516	0.934527	1.145936	0.611086	4.209246
Dy	26	10.02132	16.94024	17.30033	24.29679	25.51377	11.39979	6.01813	9.293642	4.499064	22.8682
Ho	27	2.004046	3.896247	3.572645	5.166134	4.814819	1.913911	1.002434	1.778485	0.855646	3.329332
Er	28	6.337074	12.31718	11.30851	15.28769	13.77223	4.827029	2.52161	4.560637	2.136547	6.876914
Tm	29	1.10467	2.10082	1.813117	2.436685	2.125164	0.724649	0.366644	0.599429	0.336232	0.793508
Yb	30	6.917274	12.8799	10.83266	14.34507	12.71166	3.688604	2.043858	3.45659	1.74294	3.485918
Lu	31	0.308853	0.475267	0.424928	0.488647	0.431642	0.297362	0.267217	0.301179	0.258396	0.299407
Hf	32	0.784182	0.966001	0.98593	0.962868	1.025675	0.752245	0.667481	0.804545	0.603258	0.476677
Ta	33	0.340816	0.86368	1.137305	0.842543	0.75271	0.677335	0.377287	0.391783	0.251007	0.332994
W	34	0.246861	0.31315	0.327604	0.36409	0.325026	0.339849	0.270906	0.278998	0.277981	0.285857
Pb	35	8.741885	4.039791	3.866154	9.944472	4.909411	2.168341	2.398294	2.812825	2.034703	2.54175
Th	36	0.671883	0.456367	0.369899	0.805723	0.420173	0.253698	0.179569	0.143387	0.115486	0.165671
U	37	0.306506	0.417314	0.390437	0.435495	0.399786	0.399688	0.38513	0.413572	0.363549	0.395428

Appendix 4: P-T Calculations using 9 averaged garnet values, 32 omphacite points, and 21 phengite points.

	Host 1	Host 1	Host 1	Host 1	Host 1	Host 1	Host 1	Host 1	Host 1
Comment	Omp 2, Phg 2	Omp 2, Phg 3	Omp 2, Phg 4	Omp 3, Phg 2	Omp 3, Phg 3	Omp 3, Phg 4	Omp 4, Phg 2	Omp 4, Phg 3	Omp 4, Phg 4
T(K)	923	923	923	812	812	812	1232	1231	1233
T(C)	650	650	650	539	539	539	959	958	960
P(KBAR)	33.04	32.93	33.09	28.48	28.39	28.53	64.68	64.48	64.81
	Host 1b	Host 1b	Host 1b	Host 1b	Host 1b	Host 1b	Host 1b	Host 1b	Host 1b
Comment	Omp 5, Phg 5	Omp 5, Phg 6	Omp 5, Phg 7	Omp 6, Phg 5	Omp 6, Phg 6	Omp 6, Phg 7	Omp 7, Phg 5	Omp 7, Phg 6	Omp 7, Phg 7
T(K)	1876	1896	1946	631	639	644	1033	1056	1071
T(C)	1603	1623	1673	358	366	371	760	783	798
P(KBAR)	99.79	101.12	107.44	19.03	21.13	22.42	36.34	40.31	42.81
	Host 2	Host 2	Host 2	Host 2	Host 2	Host 2	Host 2	Host 2	Host 2
Comment	Omp 56, Phg 8	Omp 56, Phg 9	Omp 56, Phg 10	Omp 59, Phg 8	Omp 59, Phg 9	Omp 59, Phg 10	Omp 60, Phg 8	Omp 60, Phg 9	Omp 60, Phg 10
T(K)	1464	1474	1432	857	860	847	1391	1399	1361
T(C)	1191	1201	1159	584	587	574	1118	1126	1088
P(KBAR)	67.50	68.91	62.78	25.85	26.46	23.72	68.89	70.18	64.28
	Host 3	Host 3	Host 3	Host 3	Host 3	Host 3			
Comment	Omp 18, Phg 11	Omp 18, Phg 13	Omp 20, Phg 11	Omp 20, Phg 13	Omp 22, Phg 11	Omp 22, Phg 13			
T(K)	742	724	1764	1661	1006	973			
T(C)	469	451	1491	1388	733	700			
P(KBAR)	23.75	19.57	97.18	82.94	42.21	35.87			
	Host 4	Host 4	Host 4	Host 4	Host 4	Host 4			
Comment	Omp 25, Phg 14	Omp 25, Phg 16	Omp 26, Phg 14	Omp 26, Phg 16	Omp 27, Phg 14	Omp 27, Phg 16			
T(K)	1115	1119	956	959	947	949			
T(C)	842	846	683	686	674	676			
P(KBAR)	38.13	38.78	30.10	30.63	29.85	30.35			
	Alt 1	Alt 1	Alt 1	Alt 1	Alt 1	Alt 1			
Comment	Omp 30, Phg 17	Omp 30, Phg 19	Omp 33, Phg 17	Omp 33, Phg 19	Omp 34, Phg 17	Omp 34, Phg 19			
T(K)	710	709	714	712	699	698			
T(C)	437	436	441	439	426	425			
P(KBAR)	21.01	20.71	20.90	20.58	20.54	20.24			
	Alt 2	Alt 2	Alt 2	Alt 2	Alt 2	Alt 2	Alt 2	Alt 2	
Comment	Omp 35, Phg 20	Omp 35, Phg 22	Omp 37, Phg 20	Omp 37, Phg 22	Omp 38, Phg 20	Omp 38, Phg 22	Omp 39, Phg 20	Omp 39, Phg 22	
T(K)	903	903	986	986	795	795	857	857	
T(C)	630	630	713	713	522	522	584	584	
P(KBAR)	33.11	33.09	39.39	39.37	29.18	29.16	31.46	31.44	
	Alt 3	Alt 3	Alt 3	Alt 3	Alt 3	Alt 3	Alt 3	Alt 3	
Comment	Omp 40, Phg 24	Omp 40, Phg 25	Omp 41, Phg 24	Omp 41, Phg 25	Omp 42, Phg 24	Omp 42, Phg 25	Omp 43, Phg 24	Omp 43, Phg 25	
T(K)	714	711	894	889	820	817	1101	1094	
T(C)	441	438	621	616	547	544	828	821	
P(KBAR)	21.30	20.71	34.64	33.79	27.54	26.84	43.90	42.80	
	Alt 4	Alt 4	Alt 4	Alt 4	Alt 4	Alt 4	Alt 4	Alt 4	Alt 4
Comment	Omp 45, Phg 26	Omp 45, Phg 32	Omp 46, Phg 26	Omp 46, Phg 32	Omp 47, Phg 26	Omp 47, Phg 32	Omp 48, Phg 26	Omp 48, Phg 32	Omp 49, Phg 26
T(K)	740	747	1098	1113	653	658	760	767	1550
T(C)	467	474	825	840	380	385	487	494	1277
P(KBAR)	22.27	23.70	48.12	50.78	20.28	21.55	24.20	25.72	79.11

Appendix 5: Preferred trace element values for GeoReM BHVO-2 standard.

Element	Li	Sc	V	Cr	Ni	Cu	Zn	Rb	Sr	Y	Zr	Nb
Preffered Value (µg/g)	4.5	31.83	318.2	287.2	119.8	129.3	103.9	9.261	394.1	25.91	171.2	18.1
Uncertainty (µg/g)	0.085	0.34	2.3	3.1	1.2	1.4	1	0.096	1.7	0.28	1.3	0.2
Element	Mo	Cs	Ba	La	Ce	Pr	Nd	Sm	Eu	Gd	Tb	
Preffered Value (µg/g)	4.07	0.0996	130.9	15.2	37.53	5.339	24.27	6.023	2.043	6.207	0.9392	
Uncertainty (µg/g)	0.16	0.0022	1	0.08	0.19	0.028	0.25	0.057	0.012	0.038	0.006	
Element	Dy	Ho	Er	Tm	Yb	Lu	Hf	Ta	W	Pb	Th	U
Preffered Value (µg/g)	5.28	0.9887	2.511	0.3349	1.994	0.2754	4.47	1.154	0.251	1.653	1.224	0.412
Uncertainty (µg/g)	0.028	0.0053	0.014	0.0031	0.027	0.0024	0.025	0.019	0.035	0.038	0.016	0.035

Appendix 6: Test for accuracy of the current XRF major and trace element calibration being utilized in Franklin and Marshall College X-ray laboratory using the BHVO-2 geochemical standard performed in May of 2014.

Specimen	BHVO-2/1	BHVO-2/2	BHVO-2/3	BHVO-2/4	BHVO-2/5	BHVO-2/6	BHVO-2/7
SiO2	49.94	50.02	49.97	49.94	49.83	49.95	50.00
TiO2	2.72	2.73	2.73	2.72	2.72	2.73	2.73
Al2O3	13.63	13.66	13.66	13.65	13.61	13.62	13.65
Fe2O3T	12.43	12.45	12.41	12.42	12.40	12.43	12.42
MnO	0.165	0.165	0.165	0.165	0.165	0.165	0.164
MgO	7.299	7.292	7.285	7.294	7.291	7.309	7.304
CaO	11.473	11.482	11.485	11.490	11.473	11.505	11.491
Na2O	2.196	2.190	2.197	2.200	2.202	2.191	2.190
K2O	0.505	0.507	0.507	0.505	0.504	0.504	0.505
P2O5	0.265	0.267	0.267	0.266	0.267	0.266	0.266
Total	100.623	100.763	100.676	100.65	100.462	100.67	100.72

Appendix 7: Natural standards used to measure various oxides for clinopyroxene (cpx), phengite (phg), and garnet (grt) on the microprobe.

	Omp	Kakanui hbl	Spessartine	Microcline	Natural Grt
Cpx	Na, Fe, Ca, Al, Si	Ti, Mg	Mn	K	----------------
Phg	Na, Ca	Fe, Ti, Mg	---------------	Al, Si	----------------
Grt	Na	Ti	Mn	-------------	Si, Mg, Al, Fe

Appendix 8: Table of masses (g) for each rock powdered sample that was weighed out and prepped for trace element analysis. Sample EO1-1 to EO1-5 represents the host; Sample EO1-6 to EO1-9 represents the alteration. EO1-10 represents the vein, and EO1-11 is a BHVO-2 standard.

Lab #	TH1	TH2	TH3	TH4	TH5	TH6	TH7	TH8	TH9	TH10	TH11	Blank
Sample #	EO1-1	EO1-2	EO1-3	EO1-4	EO1-5	EO1-6	EO1-7	EO1-8	EO1-9	EO1-10	EO1-11	N/A
Mass (g)	0.02561	0.01937	0.02043	0.02049	0.01987	0.02079	0.02042	0.01967	0.02089	0.01958	0.01985	0

Appendix 9: Ternary plot data

Appendix 9a: Data used for garnet ternary plot using Host 1-4 and Alt 1-5 averages.

Garnet	Fe	Mg	Ca+Mn
Host1	66.5912507	21.8634356	11.5453137
Host1b	66.9924334	22.6621004	10.3454662
Host2	65.4465952	20.154158	14.3992468
Host3	66.5854605	19.2139007	14.2006388
Host4	66.670643	22.2190739	11.110283
Alt1	64.9857676	24.2661933	10.7480391
Alt2	65.546385	23.011722	11.441893
Alt3	67.706698	20.1252677	12.1680343
Alt4	65.2854758	24.0723806	10.6421436
Alt5	66.0486169	23.4021815	10.5492016

Appendix 9b: Data used for omphacite ternary plot using all acceptable host and alteration points.

Omphacite	Ca+Mg+Fe2+	Na+Al	Al+Fe3+
Host2	17.656	51.41	30.934
host3	17.839	51.411	30.75
host4	8.39	57.85	33.76
host5	8.98	57.11	33.91
host6	26.28	46.02	27.7
host7	17.31	51.81	30.88
host18	15.73	54.05	30.22
host20	7.33	58.98	33.69
host22	10.33	57.05	32.62
host25	18.2	51.35	30.45
host26	20.7	49.7	29.6
host27	21.64	49.48	28.88
host56	10.56	58.79	30.65
host59	21.13	51.34	27.53
host60	8.53	58.89	32.58
Alt30	41.21	37.57	21.22
Alt33	35.38	41.28	23.34
Alt34	39.52	38.84	21.64
Alt35	17.94	52.01	30.05
Alt37	14.72	53.69	31.59
Alt38	16.58	52.65	30.77
Alt39	17.61	51.9	30.49
Alt40	27.48	46.33	26.19
Alt41	12.31	55	32.69
Alt42	17.74	52.08	30.18
Alt43	13.35	54.41	32.24
Alt45	32.02	43.23	24.75
Alt46	10.92	55.92	33.16
Alt47	25.07	47.64	27.29
Alt48	23.13	49.04	27.83
Alt49	8.39	56.88	34.73

Appendix 10: BSE image of host assemblage 1 depicting garnet, omphacite, and phengite used for P-T calculations. Numbers match those in the raw microprobe data table in Appendix 1.